GeoArabia, v. 14, no. 4, 2009, p. 17-48
Gulf PetroLink, Bahrain

Opening of the Neo-Tethys Ocean and the Pangea B to Pangea A transformation during the Permian

Giovanni Muttoni, Maurizio Gaetani, Dennis V. Kent, Dario Sciunnach, Lucia Angiolini, Fabrizio Berra, Eduardo Garzanti, Massimo Mattei and Andrea Zanchi

ABSTRACT

We studied the stratigraphy, composition, and paleomagnetic properties of lateritic weathering profiles of Permian age from northern Iran and western Karakoram, Pakistan. A limited set of samples deemed representative yielded stable low-inclination paleomagnetic components carried essentially by hematite of chemical origin isolated in massive, fine-grained, and homogeneous ferricrete facies. These laterites originated at equatorial paleolatitudes characterized by intense weathering processes under warm and humid climatic conditions. Paleomagnetic estimates of paleolatitude from Iran, Karakoram, and north Tibet from this study and the literature, albeit sparse, provide testable constraints on the motion of the Cimmerian terranes as the result of the opening of the Neo-Tethys Ocean along the eastern margin of Gondwana during the Permian. We confirm and help refine previous suggestions that the Cimmerian terranes migrated from southern Gondwanan paleolatitudes in the Early Permian to subequatorial paleolatitudes by the Middle Permian – Early Triassic. As a novel conclusion, we find that timing, rates, and geometry of Cimmerian tectonics are broadly compatible with the transformation of Pangea from an Irvingian B to a Wegenerian A-type configuration with Neo-Tethyan opening taking place contemporaneously essentially in the Permian.

INTRODUCTION

The Late Paleozoic – Early Mesozoic was a period of major plate tectonic reconfiguration. Gondwana and Laurasia completed Variscan assemblage into one supercontinent, Pangea, and subsequently the Neo-Tethys Ocean opened along the eastern margin of Gondwana while the Paleo-Tethys Ocean underwent subduction along the southern margin of Eurasia. A strip of Gondwanan terranes, hereafter termed Cimmerian terranes and including, among others, Iran (Figures 1 and 2, IR), Afghanistan (A), Karakoram (KK), and Qiangtang (QT), broke off from the eastern margin of Gondwanan, drifted northward across the Paleo-Tethys Ocean, and eventually collided with the Eurasian margin, giving birth to a conspicuous mountain chain, the Cimmerian Orogen (e.g. Sengör, 1979; Dercourt et al., 1993; Van der Voo, 1993; Besse et al., 1998; Metcalfe, 2006; Ruban et al., 2007; Muttoni et al., 2009).

Several aspects of this plate-tectonic scenario are, however, still uncertain insofar as timing and rates of motion of several Cimmerian terranes are poorly constrained (see the comprehensive review of Van der Voo, 1993). This is essentially because paleomagnetic-based estimates of paleolatitude obtained with modern techniques are extremely scanty for these tectonically complex terranes. For example, in the current version of the Global Paleomagnetic Database, only nine reliable paleomagnetic poles (defined by paleomagnetic components retrieved from fully demagnetized samples by means of least-square analysis) are listed for Iran, a country c. 1.6×10^6 km^2 in size and composed of several tectonic units, e.g. Alborz, Central Iran, Sanandaj-Sirjan (Figure 1). No paleomagnetic data whatsoever are available for Afghanistan, a country largely comprised of the rather poorly studied Helmand and Farah tectonic units (Figure 1). Pakistan, c. 0.8×10^6 km^2 in size, yielded thus far 30 reliable paleomagnetic entries, only four of which relate, however, to rocks older than ca. 200 Ma, and none of which pertain to the Karakoram Terrane in northern Pakistan (Figure 1). A total of 12 reliable entries are listed for the Qiangtang Terrane of north Tibet, only two of which, however, relate to rocks older than ca. 200 Ma. As a comparison, Italy, c. 0.3×10^6 km^2 in size (c. 1/5 the size of Iran), provided thus far 61 reliable entries; that is to say, Italy is known from a paleomagnetic viewpoint c. 8.5 times better than Iran.

Figure 1: Present-day distribution of main Cimmerian terranes amid Gondwanan and Eurasian plates (adapted from Torsvik and Cocks, 2004; Ruban et al., 2007). Those Cimmerian terranes discussed in this study are Iran (comprised of NW Iran, Alborz, Central Iran, and Sanandaj-Sirjan), Afghanistan (Helmand and Farah), Karakoram in northern Pakistan, and Qiangtang in North Tibet. Note that Karakoram in northern Pakistan is Cimmerian and di fferent from the Hunic Karakum-Turan Terrane.

Another subject of debate is the relative position of the major plates that constituted Pangea during the Late Paleozoic – Early Mesozoic. According to several authors, Pangea was always similar to the archetypal Wegenerian configuration known as Pangea A, with South America and Africa placed south of North America and Europe (e.g. Van der Voo, 1993; Scotese, 2001; Stampfli and Borel, 2002; Ziegler et al., 2003; Torsvik and Cocks, 2004) (Figure 2a). However, Irving (1977) suggested that Pangea evolved into a Wegenerian A-type configuration from an initial B configuration where South America and Africa were placed south of Europe and Asia, as suggested later also by other authors (Morel and Irving, 1981; Muttoni et al., 1996; Torq et al., 1997; Bachtadse et al., 2002; Muttoni et al., 2003, 2004; Angiolini et al., 2007). According to Irving (1977) and Torq et al. (1997), the transformation by means of dextral motion of Laurasia relative to Gondwana occurred sometime during the Triassic, whereas according to Muttoni et al. (2003, 2004), the transformation was completed by the Late Permian – Early Triassic and was largely coeval to the opening of the Neo-Tethys Ocean (Figures 2b and c). Muttoni et al. (2003, 2004) suggested the existence of a plate circuit where the Gondwanan Plate was bounded to the east by the Neo-Tethyan ridge, to the north along the former Variscan Suture by a zone of (diffused) dextral shear, and to the west along South America by the subduction of the Panthalassa Ocean (Figures 2b and c). These authors further suggested that the Pangea B to Pangea A transformation was coeval with the onset of northward drift of the Cimmerian terranes across the Paleo-Tethys by way of Neo-Tethys opening, depicting altogether an internally consistent plate motion scenario that is the subject of this study.

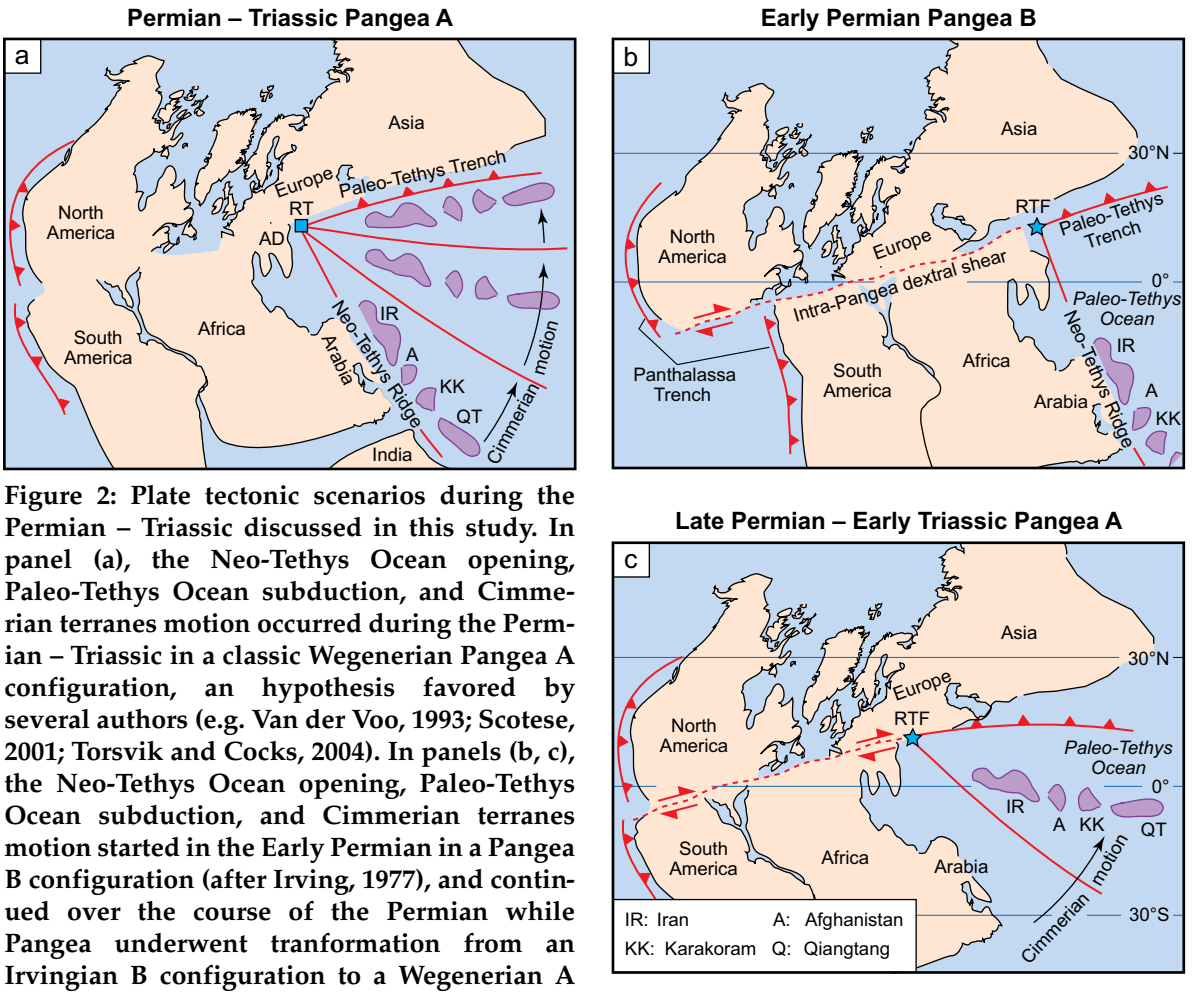

Figure 2: Plate tectonic scenarios during the Permian – Triassic discussed in this study. In panel (a), the Neo-Tethys Ocean opening, Paleo-Tethys Ocean subduction, and Cimmerian terranes motion occurred during the Permian – Triassic in a classic Wegenerian Pangea A configuration, an hypothesis favored by several authors (e.g. Van der Voo, 1993; Scotese, 2001; Torsvik and Cocks, 2004). In panels (b, c), the Neo-Tethys Ocean opening, Paleo-Tethys Ocean subduction, and Cimmerian terranes motion started in the Early Permian in a Pangea B configuration (after Irving, 1977), and continued over the course of the Permian while Pangea underwent tranformation from an Irvingian B configuration to a Wegenerian A configuration (Muttoni et al., 2003, 2004). IR is Iran (NW Iran, Alborz, Central Iran, and Sanandaj-Sirjan; see also Figure 1); A is Afghanistan (Helmand and Farah); KK is Karakoram in northern Pakistan; QT is Qiangtang in north Tibet. See text for discussion. Reconstruction made with Paleo-Mac (Cogné, 2003).

Here we attempt to better define the history of motion of the Cimmerian terranes as a consequence of the opening of the Neo-Tethys Ocean by presenting stratigraphic data and paleomagnetically determined estimates of paleolatitude for northern Iran and western Karakoram, Pakistan. These data, in conjunction with literature data from additional Cimmerian terranes, are used to gauge the compatibility of the Neo-Tethyan opening in terms of timing and rates with the inferred plate transformation of Pangea B to Pangea A during the Permian.

STRATIGRAPHY

We conducted stratigraphic and paleomagnetic analyses on lateritic sequences (laterites) from northern Iran and western Karakoram that seemingly resulted from intensive and long-lasting weathering processes of the underlying parent rocks under warm and humid climate conditions typical of intertropical-equatorial paleolatitudes. In particular, we focused paleomagnetic analyses on fine-grained and homogeneous ferricrete facies. The reason why we did so is that several studies from the literature showed the reliability of such fine-grained, homogeneous, and non-reworked ferricretes as recorders of paleomagnetic directions (Idnurm and Senior, 1978; Schmidt et al., 1983; Schmidt and Ollier, 1988; Acton and Kettles, 1996). Moreover, estimates of paleolatitude determined from paleomagnetic components retrieved from fine-grained and homogeneous ferricretes should, in principle, not be biased by inclination flattening, which can occur in sediments when the remanent magnetization is acquired by detrital processes involving platy hematite grains (e.g. King and Rees,

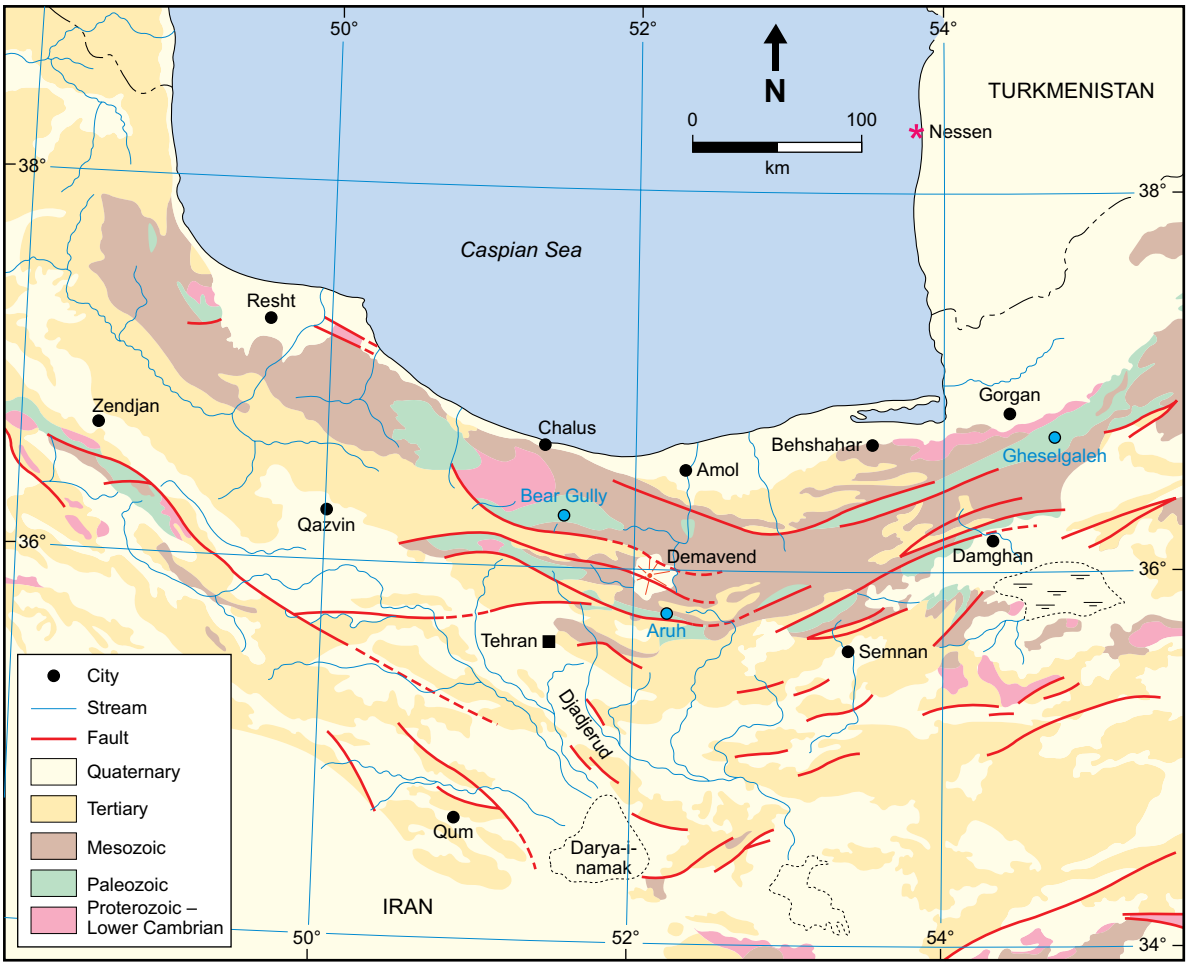

Figure 3: Geological sketch map of the Alborz Mountains in north Iran. The Aruh section is located at N35°39'43.5", E52°24'16.0". Also indicated are the broadly coeval Bear Gully and Gheselgaleh sections.

1966; Tauxe and Kent, 1984). This is because the hematite contained in ferricretes is a chemically precipitated product of the weathering process. It therefore carries a chemical remanent magnetization rather than a detrital remanent magnetization, as observed for example in detailed paleomagnetic and magnetostratigraphic studies on Cenozoic lateritic profiles from French Guiana and Suriname (Théveniaut and Freyssinet, 1999; 2002). Finally, lateritization is a long-lasting process that can even span more than one polarity reversal of the Earth's magnetic field (e.g. Schmidt and Embleton, 1976; Théveniaut and Freyssinet, 2002). Therefore, secular variation should be averaged out even in relatively thin lateritic profiles, making paleomagnetic estimates of paleolatitude a close proxy of the true average latitude of lateritization.

Alborz Mountains, Northern Iran

A lateritic profile near the Aruh village in the Alborz Mountains (N35°39'43.5'', E52°24'16.0''; Figure 3) is underlain by carbonate platform limestones of the Ruteh Formation and overlain by those of the Elikah Formation (Assereto, 1963; Glaus, 1964; Zaninetti et al., 1972; Seyed-Emami, 2003) (Figures 4 and 5). The sedimentary sequence is located along the southern flank of an upper Cenozoic anticline intersected by the active Mosha left-lateral, strike-slip fault, and has been tilted to nearly vertical, essentially during the Cenozoic (e.g. Allen et al., 2003), although the effects of older deformational phases since the Late Triassic – Early Jurassic Cimmerian Orogeny cannot be excluded. The lateritic profile consists of the following stratigraphic units, from base to top:

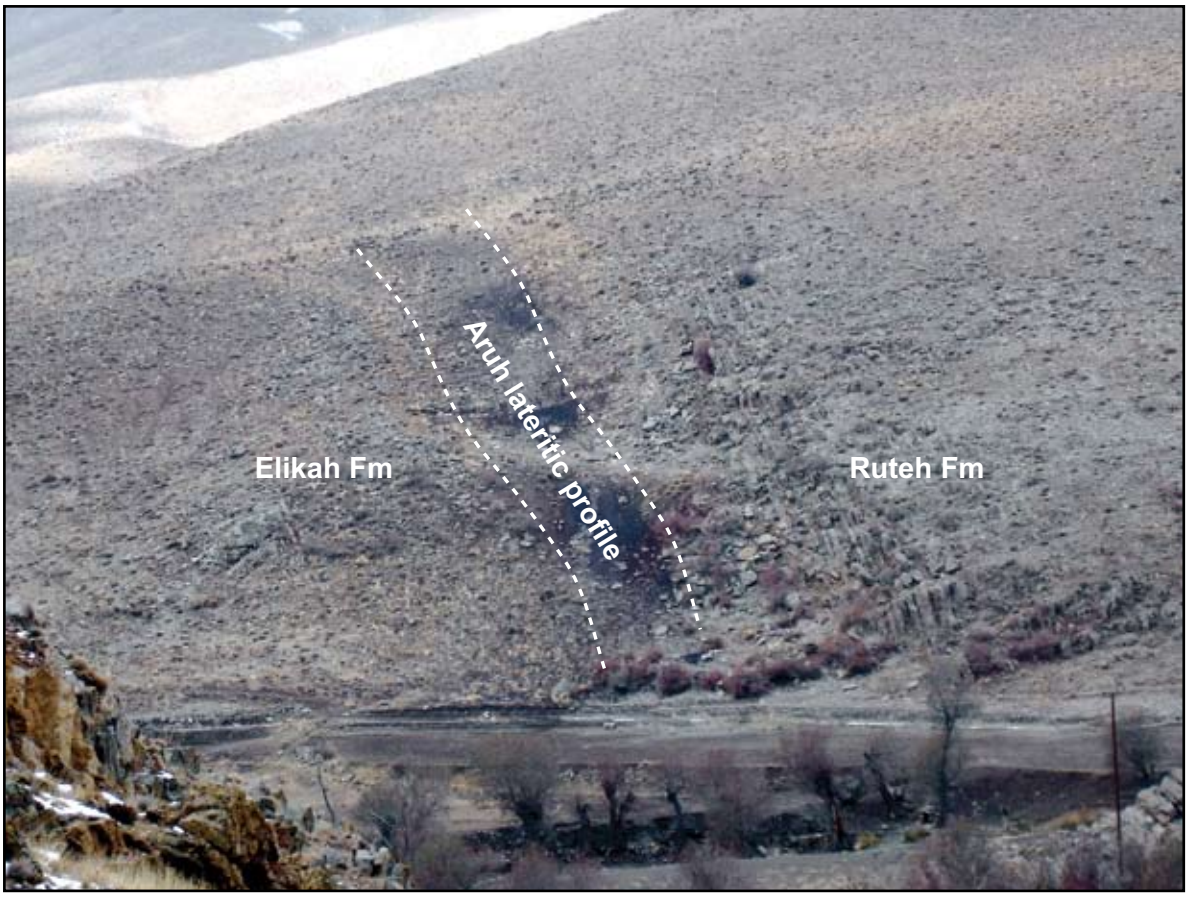

Figure 4: Photograph of the Aruh lateritic profile, stratigraphically comprised between the Ruteh Formation below, and the Elikah Formation above (the section is slightly overturned). The Aruh ferricrete bed, sampled for paleomagnetic analyses, crops out in the middle part of the Aruh lateritic profile. Width of scene c. 100 m.

Aruh Unit 1: The lowermost c. 1 m consists of quartz-rich conglomerates grading upwards into quartzarenites and lying with sharp planar contact, locally marked by a silicified horizon, directly on top of the Ruteh Formation (Figure 6). Sedimentary structures (cross laminations, erosional surfaces) suggest a fluvial origin for these sediments. Thin section analyses revealed that the well-sorted quartzarenites contain generally rounded monocrystalline quartz grains (mQz, Figure 7a and b), less frequently polycrystalline grains (pQz, Figures 7a and b). A reddish shaly matrix fills the intergranular porosity (m, Figures 7a and b).

Aruh Unit 2: Above follow c. 16 m of yellowish to brown laminated marls and, toward the top, fine-grained oolitic limestones with low-angle cross laminations. A 3–5 m-thick red-brown, fine-grained, homogeneous, and massive bed, hereafter referred to as Aruh ferricrete (Figure 5), occurs in this interval. Scanning Electron Microscopy (SEM), in combination with energy dispersive spectrometry (EDS), revealed that the Aruh ferricrete contains pisoids (Figure 7c) immersed in abundant fine-grained matrix rich in Fe and Al oxides (Figures 7d and e). The most homogeneous portions of the Aruh ferricrete were chosen for paleomagnetic sampling.

Aruh Unit 3: At the top, the lateritic profile grades into laminated and burrowed marls and limestones rich in gastropods and oolites of the basal Elikah Formation ("calcaires vermiculè" of Zaninetti et al., 1972).

The age of the Aruh lateritic profile is based on biostratigraphic data and by comparison with correlative sections from the literature (Figure 8). The base of the overlying Elikah Formation is Induan (earliest Triassic) in age according to benthic foraminifera biostratigraphy (Zaninetti et al., 1972; Gaetani et al.,

Figure 5: Photograph of the Aruh lateritic profile, stratigraphically comprised between the Ruteh Formation below and the Elikah Formation above (the section is subvertical). The Aruh ferricrete, sampled for paleomagnetic analyses, stand out as a massive bed in a more eroded landscape. Height of cliff at distance c. 15 m.

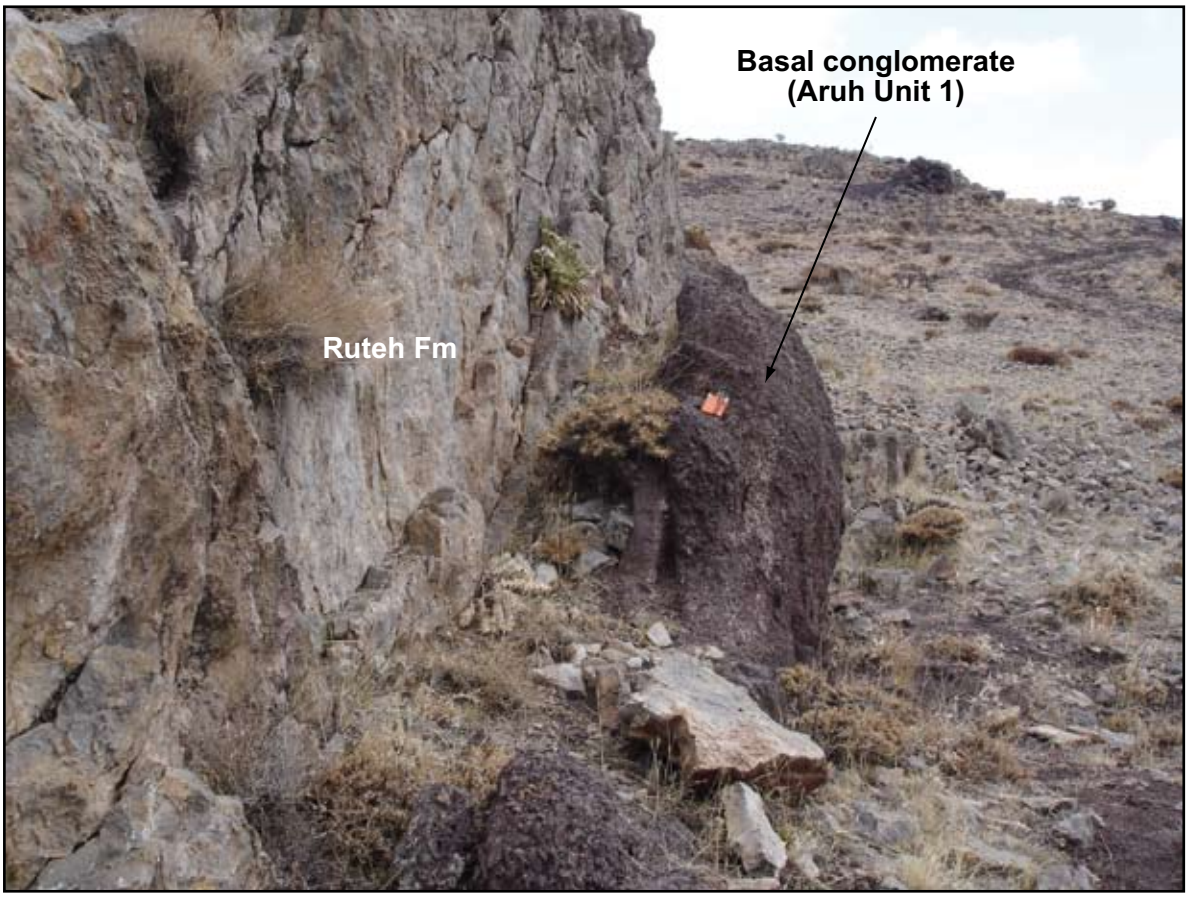

Figure 6: Photograph of the basal conglomerate-quartzarenite package (Aruh Unit 1) of the Aruh lateritic profile. Width of scene c. 4 m.

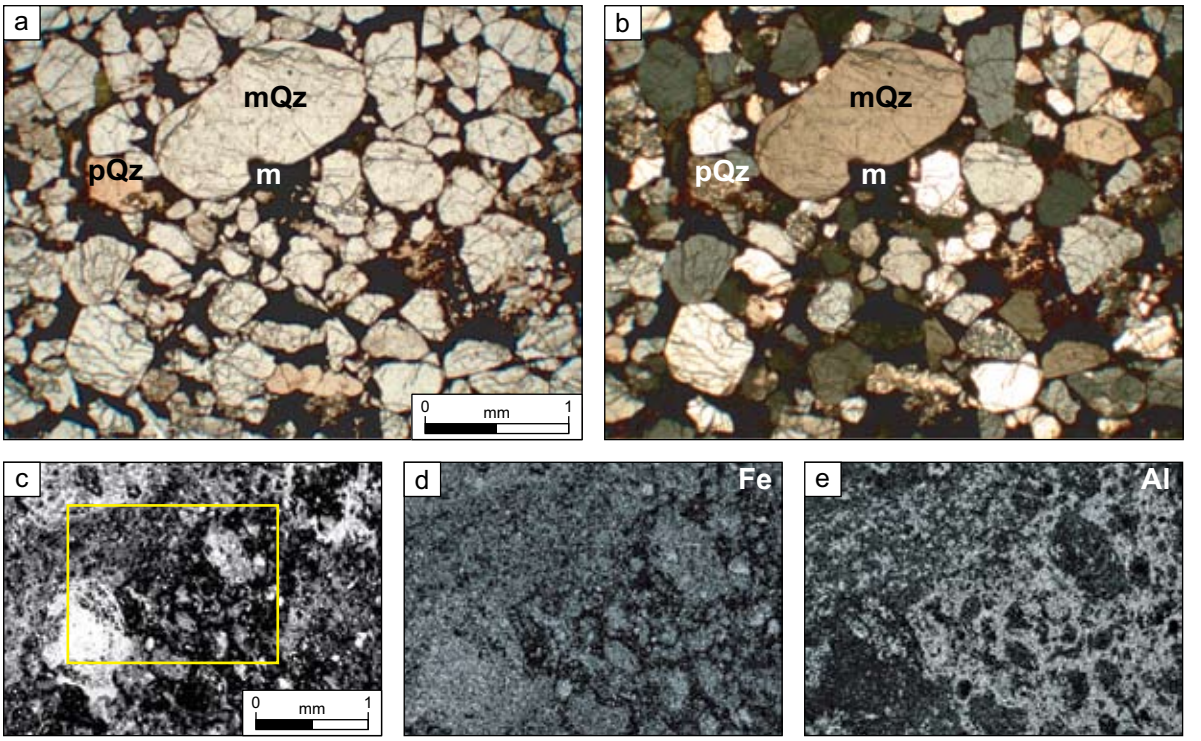

Figure 7: Thin section photographs of the basal quartzarenite (Aruh Unit 1) in parallel nicols (a) and cross-nicols (b); mQz–monocrystaline quartz, pQz–polycrystalline quartz, m–reddish shaly matrix. SEM microphotograph of a representative sample from the Aruh ferricrete bed within Aruh Unit 2 (c). Element map of the same sample (framed area in panel (c): Fe map (d) and Al map (e) (the darker the map, the higher the metal concentration).

2009). The age of the base of the lateritic profile is not well constrained at Aruh owing to the paucity of age-diagnostic fossils in the underlying Ruteh Formation. At the Bear Gully section to the northwest of Aruh (Figure 3), a lateritic profile is present between the upper part of the Ruteh Formation of Capitanian (late Middle Permian) age and the lower part of the Nesen Formation, consisting of shales, nodular limestones, and cherty limestones of Wuchiapingian (early Late Permian) age (Glaus, 1964; Gaetani et al., 2009) (Figure 8).

To the northeast of Aruh, in the Gheselgaleh (Qezelqal'eh) section (reinterpreted after Jenny and Stampfli, 1978) (Figure 3), lateritic profiles occur in the Gheshlagh (Qeshlaq) Formation. This formation consists mainly of fluvial quartzarenites resting on top of the Ruteh Formation, biostratigraphically constrained to the Capitanian (late Middle Permian; Gaetani et al., 2009), and overlain by the Elikah Formation of Induan (earliest Triassic) age (Altiner et al., 1980) (Figure 8). Fieldwork analysis (M. Gaetani) indicates that the Gheshlagh Formation represents the lateral equivalent of the Nesen Formation, which at Bear Gully has a Wuchiapingian (early Late Permian) age. Lateritic profiles are common in the middle and upper part of the Gheshlagh Formation, and also in its type area in the East Alborz (Jenny and Stampfli, 1978).

We conclude that several lateritic profiles punctuate the stratigraphic interval of carbonate platform deposition of the Ruteh and Elikah formations across much of the Alborz region. These lateritic profiles formed under warm-humid conditions on a continental alluvial plain (e.g. Gheshlagh Formation; basal conglomerates of the Aruh lateritic profile) subject to pedogenesis and lateritization, and passing laterally to submerged ramps of terrigenous to carbonatic sedimentation (e.g. Nesen Formation). We are tempted to correlate the basal conglomerates of the Aruh lateritic profile to the fluvial quartzarenites of the Gheshlagh Formation in the more expanded (subsiding) Gheselgaleh section, and therefore correlate the Aruh lateritic profile to one of the lateritic profiles at the top of the Gheshlagh Formation (Figure 8). Hence, fluvial sedimentation and lateritization occurred at Aruh, broadly during the Late

Permian, or ca. 260–251 Ma according to the time scale of Menning et al. (2006), and ended with the deposition of the transgressive facies of the basal Elikah Formation of earliest Triassic age.

Western Karakoram, Pakistan

We studied a lateritic profile near the Lashkargaz village in western Karakoram, Pakistan (N36°51′46″, E73°27′28″; Figures 9 and 10). The outcrop area is entirely confined within a single tectonic unit ("Lashkargaz/ Baroghil unit" of Gaetani et al., 1996; Zanchi et al., 2007) where deformation occurred since the Cretaceous. The lateritic profile, first described as an "ironstone horizon" (Hayden, 1915) and recently termed the Gharil Formation (Gaetani et al., 1995), is underlain by carbonate platform limestones of the Ini Sar Formation (Leven et al., 2007), and overlain by those of the Ailak Formation. The Gharil Formation is 20–30 m thick and traceable along strike for over 15 km on the northern slope of the Yarkhun Valley without appreciable change in facies or thickness (Figures 10 and 11). It consists of the following stratigraphic units, from base to top:

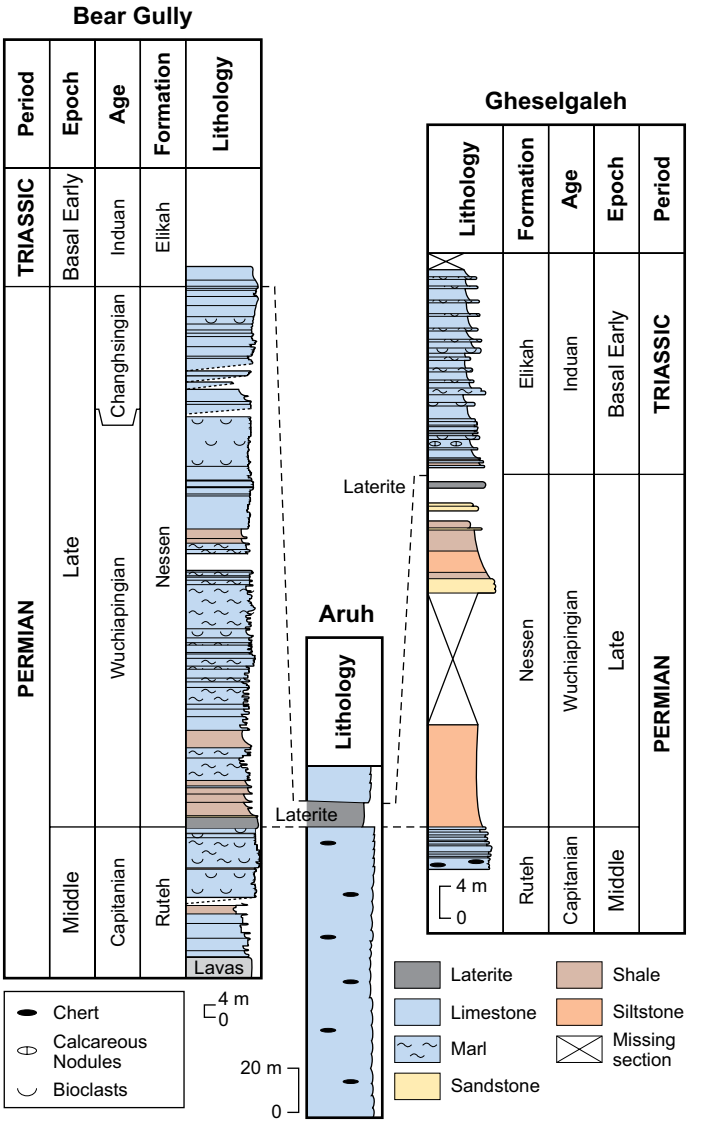

Figure 8: Correlation of the Aruh section with the broadly coeval Bear Gully and Gheselgaleh sections from the Alborz Mountains (see Figure 3 for locations).

Gharil Unit 1: A basal stratified package of conglomerates-sandstones in redbed facies, locally scouring the underlying platform carbonates of the Ini Sar Formation by as much as 7 m. The redbed facies contains pisoids reworked by traction currents and coated by kaolinite-illite clay, which is also abundant in the silty-sandy matrix (Figure 12a). Sand consists mostly of quartz grains, rounded and embayed, subordinate volcanic rock fragments displaying plagioclase laths in an oxidized groundmass, and rare feldspar consisting chiefly of microcline. Oversized, angular, and soft clasts of granule to pebble size are also present and tentatively interpreted as reworked volcanic and sedimentary intra-clasts.

Gharil Unit 2: Above follows a red-brown and massive interval. SEM/EDS observations revealed that this interval includes both homogeneous and fine-grained ferricrete facies (Figure 12b) and *in-situ* (unreworked) pisoids in a clayey-silty matrix (Figure 12c). The pisoids are made of concentric laminae of Fe-Al hydroxides (goethite, gibbsite; Table 1, columns 1-2) coating nuclei of Fe-Al hydroxides and/or clay minerals, whereas the background clayey-silty matrix consists chiefly of kaolinite and subordinate illite (Table 1, column 3). The homogeneous ferricrete facies (Figure 12b), hereafter referred to as Gharil ferricrete, was chosen for paleomagnetic sampling.

Gharil Unit 3: A second conglomerate-sandstone succession in redbed facies with similar characteristics as unit 1.

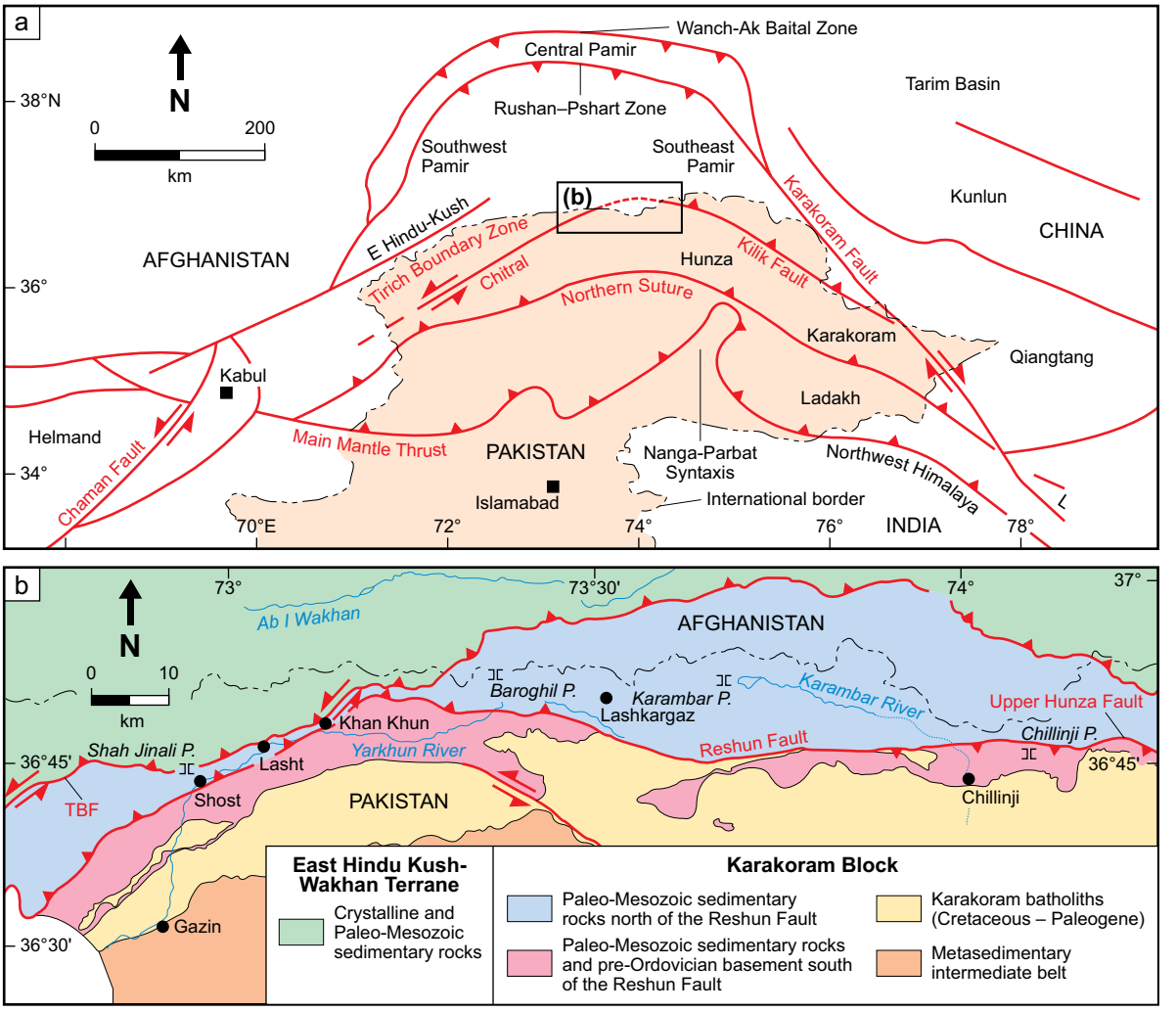

Figure 9: (a) Structural sketch map of the Karakoram and surroundings regions; the central framed area represents the outcropping area of the Lashkargaz section of this study. (b) General tectonic map of the Wakhan and Karakoram regions; the Lashkargaz section of this study is located at N36°51′46″, E73°27′28″ along the Yarkhun Valley near the Lashkargaz village (from Gaetani et al., 2004). See Figure 1 for location.

Table 1
Selected SEM-EDS microanalyses on samples from the Gharil Formation of western Karakoram, Pakistan

	1	2	3	4	5	6
SiO_2	3.69	1.18	45.39	26.29	13.01	22.16
TiO_2	0.25	0.80	0.25	0.14	3.17	0.12
Al_2O_3	76.28	1.05	33.72	23.23	7.89	19.93
Cr_2O_3	0.02	0.00	0.01	0.00	0.00	0.00
FeO_{tot}	4.36	85.65	9.70	42.49	69.38	42.64
MnO	0.07	0.08	0.02	0.01	0.05	0.00
MgO	0.18	0.04	1.92	2.35	0.68	1.55
CaO	0.05	0.07	0.01	0.05	0.03	0.04
ZnO	0.09	0.05	0.02	0.00	0.00	0.00
Na_2O	0.00	0.31	0.19	0.23	0.23	0.00
K_2O	0.04	0.05	4.49	0.52	0.96	0.28
$[H_2O]$	14.97	10.72	4.28	4.69	4.60	13.28
[Tot]	100.00	100.00	100.00	100.00	100.00	100.00

Livetime = 50 seconds, metallic cobalt for standard. Column 1 = Aluminium hydroxide (gibbsite) laminae of laterite pisoids (sample CK 99; average on 4 analyses). Column 2 = Iron hydroxide (goethite) laminae of laterite pisoids (CK 99; 2 analyses). Column 3 = Clayey (kaolinite ± illite) matrix of laterite paleosol (CK 99; 2 analyses). Column 4 = Phyllosilicate (Fe-berthierine) external laminae of ferruginous ooids (CK 206; 4 analyses). Column 5 = Opaque (iron oxide-hydroxide) external laminae of ferruginous ooids (CK 206; 4 analyses). Column 6 = Phyllosilicate (Fe-berthierine) nuclei of ferruginous ooids (CK 206; 2 analyses).

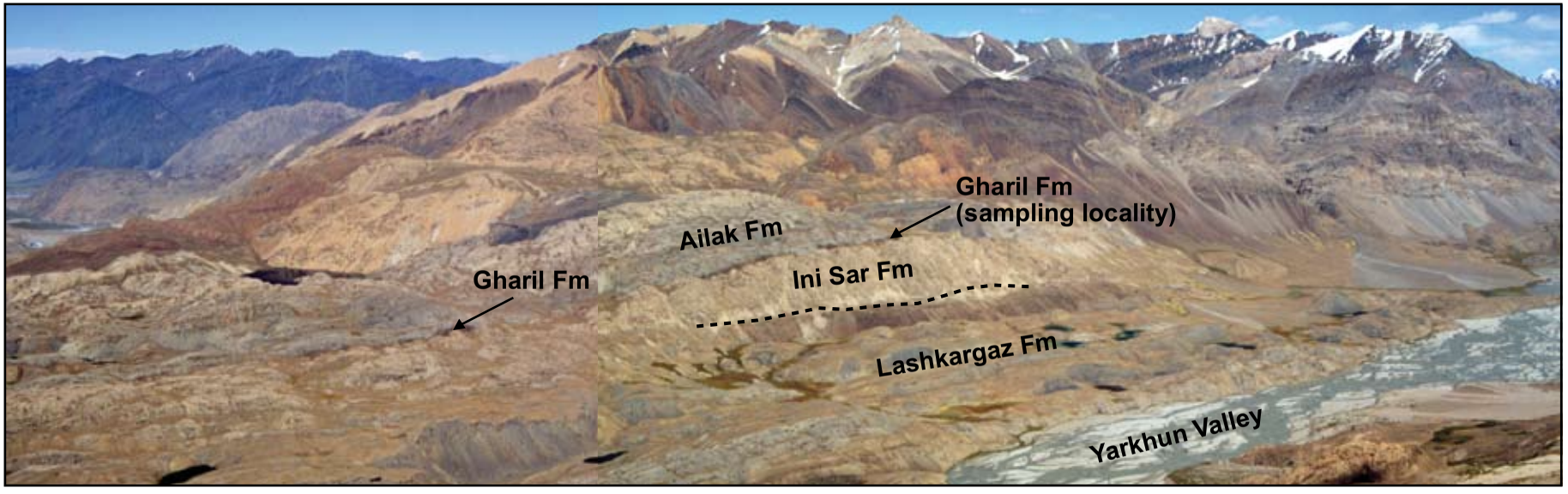

Figure 10: Composite photograph of the Yarkhun Valley near the Lashkargaz village. The Gharil Formation, target of this paleomagnetic study, is stratigraphically comprised between the Ini Sar Formation below and the Ailak Formation above, and is laterally continuous for several kilometers. The paleomagnetic sampling locality (Gharil ferricrete within the Gharil Formation) is indicated. See text for discussion. Width of scene c. 10 km.

Figure 11: Photograph of the Gharil Formation containing the Gharil ferricrete that was hand-sampled for paleomagnetic analyses. Width of scene c. 5 m.

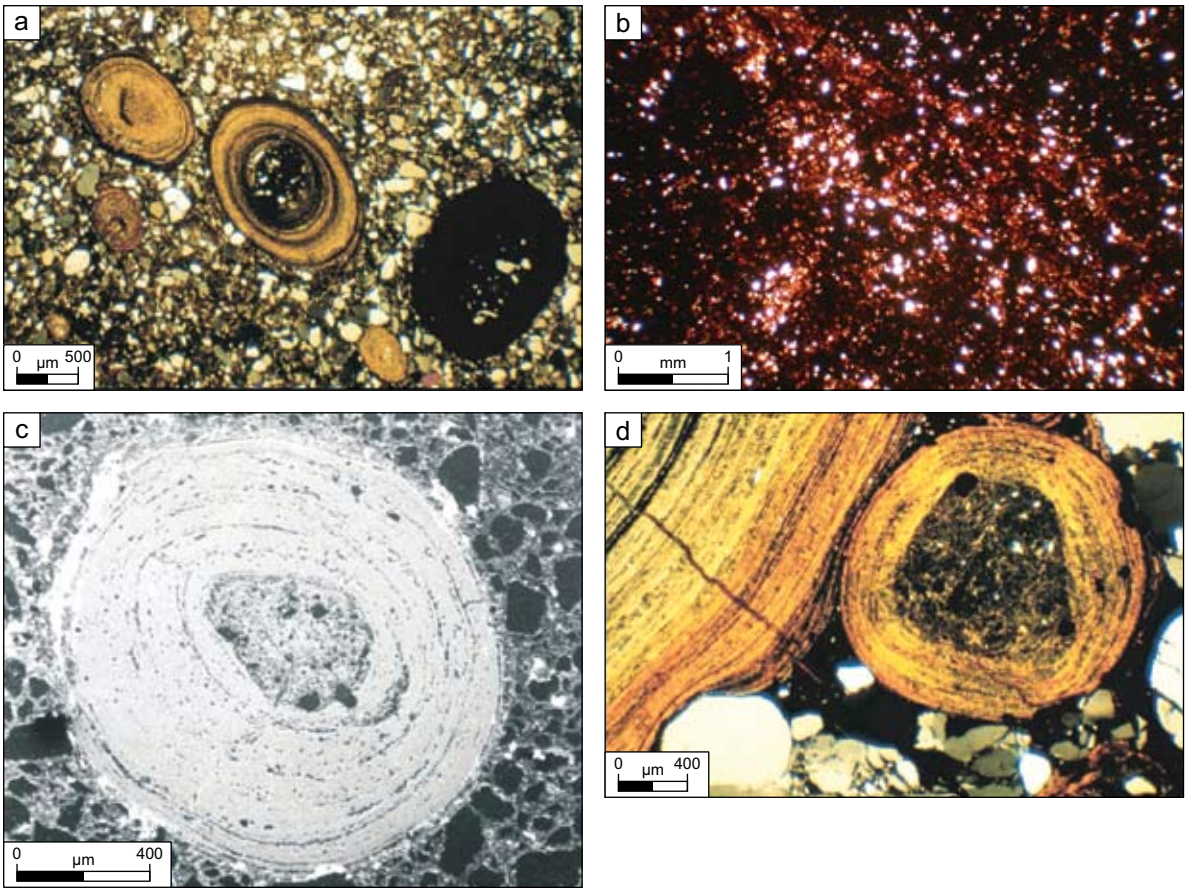

Figure 12: (a) Microphotograph (cross-nicols) of redbed facies with reworked Fe-Al pisoids (Gharil Unit 1).
(b) Microphotograph of the homogeneous Gharil ferricrete sampled for paleomagnetic anlyses (Gharil Unit 2).
(c) Back-scatter image of *in-situ* Fe-Al pisoid (Gharil Unit 2).
(d) Microphotograph (cross-nicols) of soft-shelled, ferruginous ooids and spatoliths (Gharil Unit 4).

Gharil Unit 4: Hybrid ferruginous arenites at the transition with the overlying carbonate platform limestones of the Ailak Formation. This facies is characterized by the abundance of soft-shelled ooids and spastoliths. These are made of concentric laminae of Fe-berthierine (Figure 12d; Table 1, column 4) alternating with laminae of Fe oxides-hydroxides (Figure 12d; Table 1, column 5), altogether coating nuclei made of Fe-berthierine clay clasts (Table 1, column 6) or ferriclasts. The conditions for berthierine formation (reducing chemical environment, reduced clastic input; Battacharaya, 1983) match very well the interpretation of shallow-marine transgression over pedogenized alluvial facies suggested by the sedimentary record.

The age of the Gharil Formation at Lashkargaz is based on biostratigraphic data (Figure 13). The basal part of the underlying Ini Sar Formation, c. 370 m below the Gharil Formation, is early Murgabian (ca. late Roadian, early Middle Permian) in age based on fusulinid biostratigraphy (Leven et al., 2007). The basal part of the overlying Ailak Formation is Dzhulfian (ca. Wuchiapingian, early Late Permian) in age based on benthic foraminifera biostratigraphy (Leven et al., 2007). Hence, fluvial sedimentation and lateritization occurred at Lashkargaz broadly during the middle – late part of the Middle Permian, or ca. 268–260 Ma according to the time scale of Menning et al. (2006), and ended with the deposition of the transgressive facies of the basal Ailak Formation of early Late Permian age.

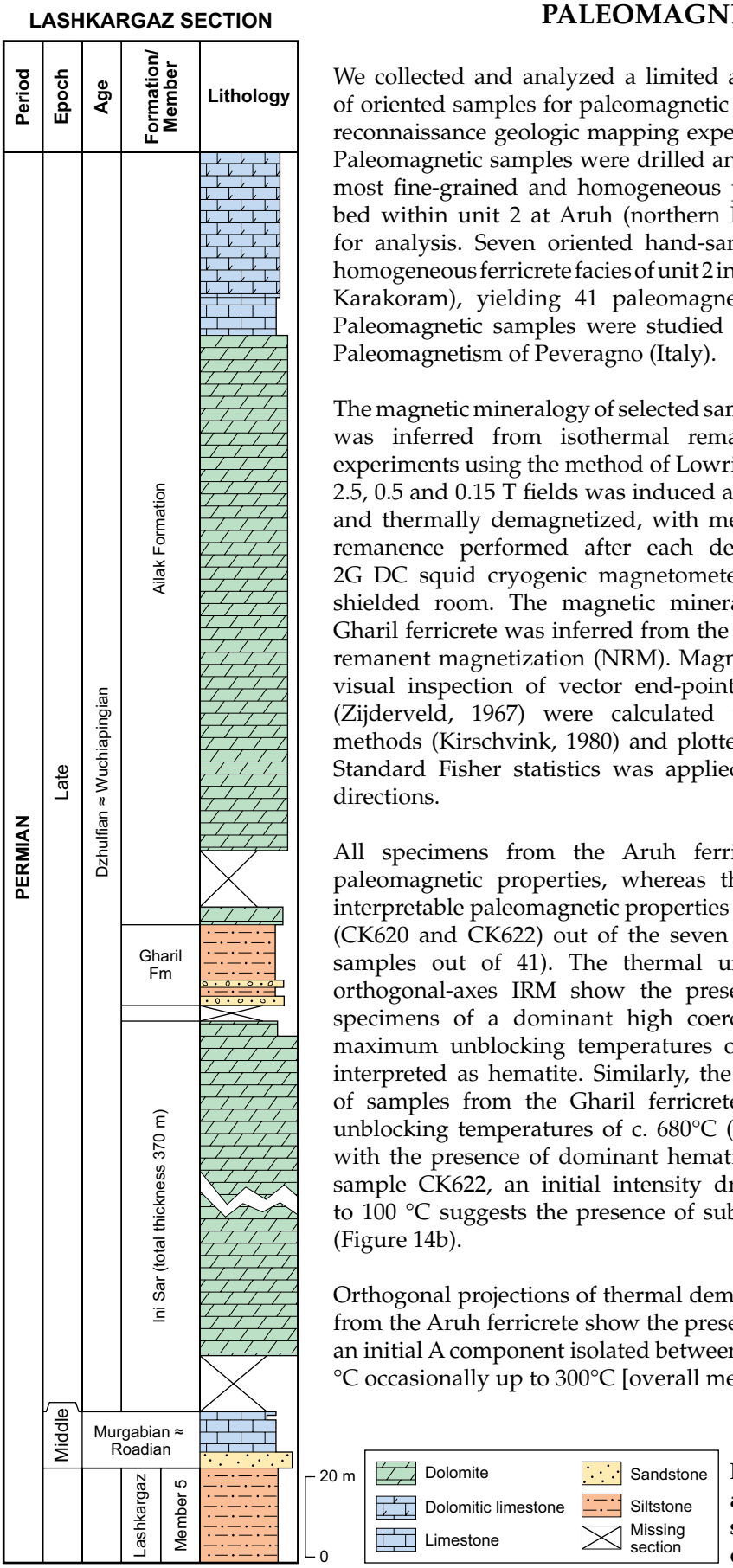

Figure 13: Stratigraphy and age of the Lashkargaz section. See text for discussion.

PALEOMAGNETISM

We collected and analyzed a limited albeit representative number of oriented samples for paleomagnetic analyses during two distinct reconnaissance geologic mapping expeditions to Iran and Pakistan. Paleomagnetic samples were drilled and oriented in the field in the most fine-grained and homogeneous parts of the massive laterite bed within unit 2 at Aruh (northern Iran), yielding 18 specimens for analysis. Seven oriented hand-samples were collected in the homogeneous ferricrete facies of unit 2 in the Lashkargaz area (western Karakoram), yielding 41 paleomagnetic specimens for analysis. Paleomagnetic samples were studied at the Alpine Laboratory of Paleomagnetism of Peveragno (Italy).

The magnetic mineralogy of selected samples from the Aruh ferricrete was inferred from isothermal remanent magnetization (IRM) experiments using the method of Lowrie (1990). A composite IRM at 2.5, 0.5 and 0.15 T fields was induced along sample orthogonal axes and thermally demagnetized, with measurements of the resultant remanence performed after each demagnetization step with a 2G DC squid cryogenic magnetometer located in a magnetically shielded room. The magnetic mineralogy of samples from the Gharil ferricrete was inferred from the thermal decay of the natural remanent magnetization (NRM). Magnetic components isolated by visual inspection of vector end-point demagnetization diagrams (Zijderveld, 1967) were calculated with standard least-square methods (Kirschvink, 1980) and plotted on equal-area projections. Standard Fisher statistics was applied to calculate overall mean directions.

All specimens from the Aruh ferricrete yielded interpretable paleomagnetic properties, whereas the Gharil ferricrete yielded interpretable paleomagnetic properties only from two hand-samples (CK620 and CK622) out of the seven collected (21 paleomagnetic samples out of 41). The thermal unblocking characteristics of orthogonal-axes IRM show the presence in the Aruh ferricrete specimens of a dominant high coercivity magnetic phase with maximum unblocking temperatures of c. 650–675°C (Figure 14a) interpreted as hematite. Similarly, the thermal decay of the NRM of samples from the Gharil ferricrete shows discrete maximum unblocking temperatures of c. 680°C (Figure 14b) again consistent with the presence of dominant hematite. In specimens from hand sample CK622, an initial intensity drop from room temperature to 100 °C suggests the presence of subsidiary amounts of goethite (Figure 14b).

Orthogonal projections of thermal demagnetization data of samples from the Aruh ferricrete show the presence in 44% of the samples of an initial A component isolated between median values of c. 100–250 °C occasionally up to 300°C [overall mean angular deviation (MAD)

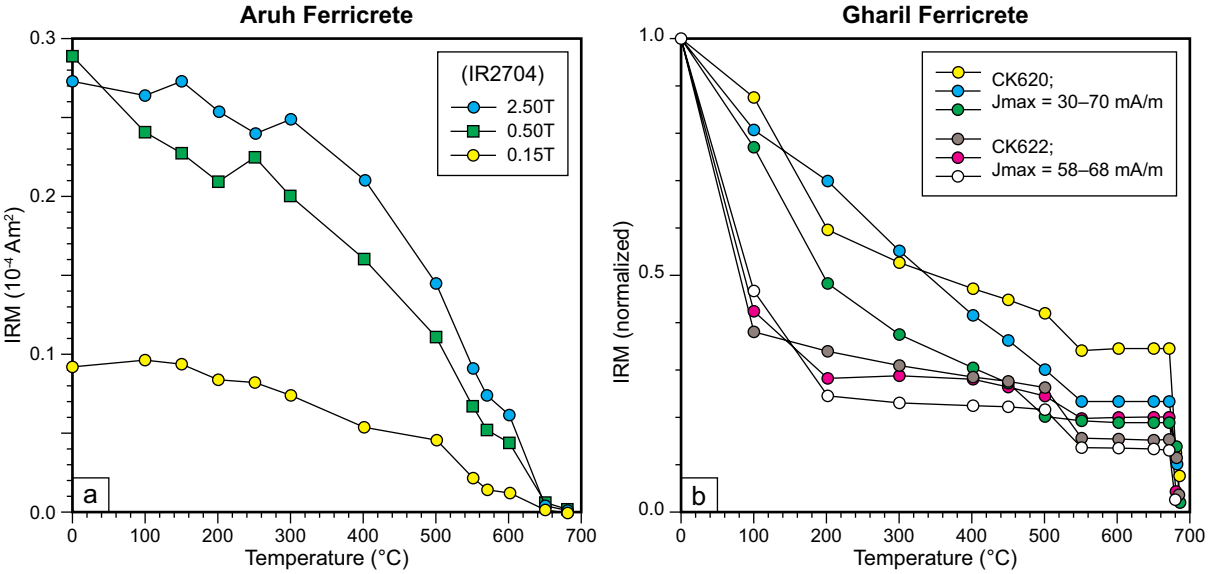

Figure 14: (a) Thermal decay of a three-component isothermal remanent magnetization (IRM) imparted at 2.5, 0.5, and 0.15 T fields in a representative Aruh ferricrete sample. (b) Thermal decay of the natural remanent magnetization (NRM) of representative Gharil ferricrete samples. All samples contain essentially hematite.

= 5.1° ± 3.9° standard deviation (SD)]. This A component is oriented north and steeply down in *in-situ* coordinates (Figure 15a, sample IR2709), whereas upon correction for bedding tilt, it acquires southerly and moderately shallow inclinations (Figure 15a, sample IR2711). The A component, with an *in-situ* overall mean direction of Dec. = 2.7°E, Inc. = 52.9° (α95 = 4.8°; Figure 15b, Table 2), is within error range aligned along a recent geocentric axial dipole field direction (GAD inclination = 54°) and is therefore interpreted as a recent overprint.

A few samples (22% of the total) show in the median temperature range c. 100–325°C up to highest values of 400°C a component direction termed B (overall MAD = 6.6° ± 1.1°SD), which is statistically steeper in *in-situ* coordinates than the GAD field (Inc. = 81.9°, α95 = 11.0°; Figure 15b, Table 2). This relatively rare B component acquires southerly and shallow negative inclinations upon correction for bedding tilt.

A well-defined characteristic (Ch) component is observed in 67% of the samples (N = 12) at higher temperatures between median values of c. 350–620°C occasionally up to 680°C (overall MAD = 4.7°±3.5° SD). This Ch component is oriented essentially west and up in *in-situ* coordinates (Figure 15a, sample IR2709; Figure 15b), and northwest and sub-horizontal upon correction for bedding tilt (Figure 15a, sample IR2711; Figure 15b). The Ch component overall mean direction in tilt corrected coordinates (Dec. = 331.8°E, Inc. = -1.3°, α95 = 10.4°; Table 2) is not compatible with any direction of Permian age expected at Aruh from the Gondwanan or Eurasian apparent polar wander path (e.g. Van der Voo, 1993; Table 2 of this study, illustrated below), and points to a paleolatitude of c. 1° (± c. 5°) either N or S. We regard the Ch component, and possibly the B component, as pre-folding ancient magnetizations acquired during lateritization processes taking place upon plate transit across equatorial paleolatitudes.

Thermal demagnetization behavior observed in specimens from hand-samples CK620 and CK622 from the Gharil ferricrete is similar to that of the Aruh ferricrete. An initial A component oriented north and steeply down in *in-situ* coordinates was isolated in 76% (N = 21) of the samples between room temperature and c. 250°C occasionally up to 400°C (overall MAD = 2.9° ± 2.1° SD; Figure 16a, samples CK620C, CK622C2). This A component has an overall mean direction of Dec. = 355.8°E, Inc. = 61.5° (α95 = 4.9°; Figure 16b, Table 2) that is statistically steeper by a few degrees than the recent field direction (GAD inclination = 55°) probably because of additional viscous overprint acquired after sampling, for example during drilling in the laboratory.

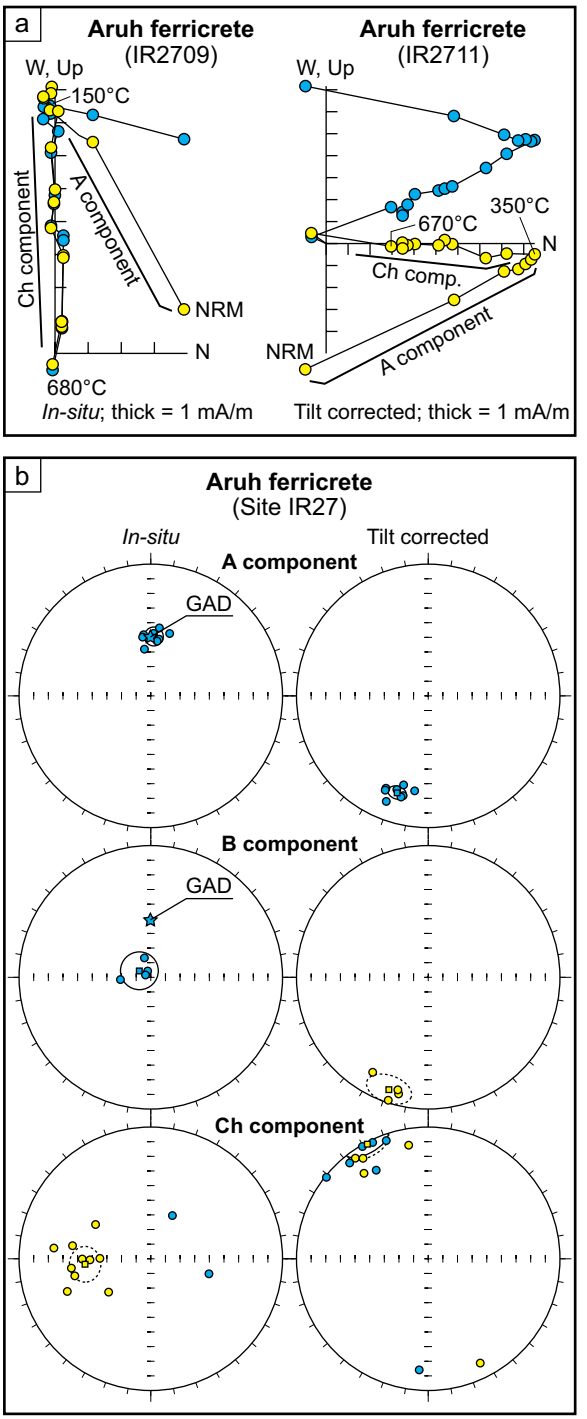

Figure 15: (a) Vector end-point demagnetization diagrams of representative samples from the Aruh ferricrete. Closed (blue) symbols are projections onto the horizontal plane and open (yellow) symbols onto the vertical plane in *in-situ* coordinates. Demagnetization temperatures are expressed in degrees centigrade ˚C. (b) Equal-area projections before (*in-situ*) and after bedding tilt correction of the characteristic component directions of the Aruh ferricrete samples. Closed (blue) symbols are projections onto the lower hemisphere and open (yellow) symbols onto the upper hemisphere. (see Table 2 for data).

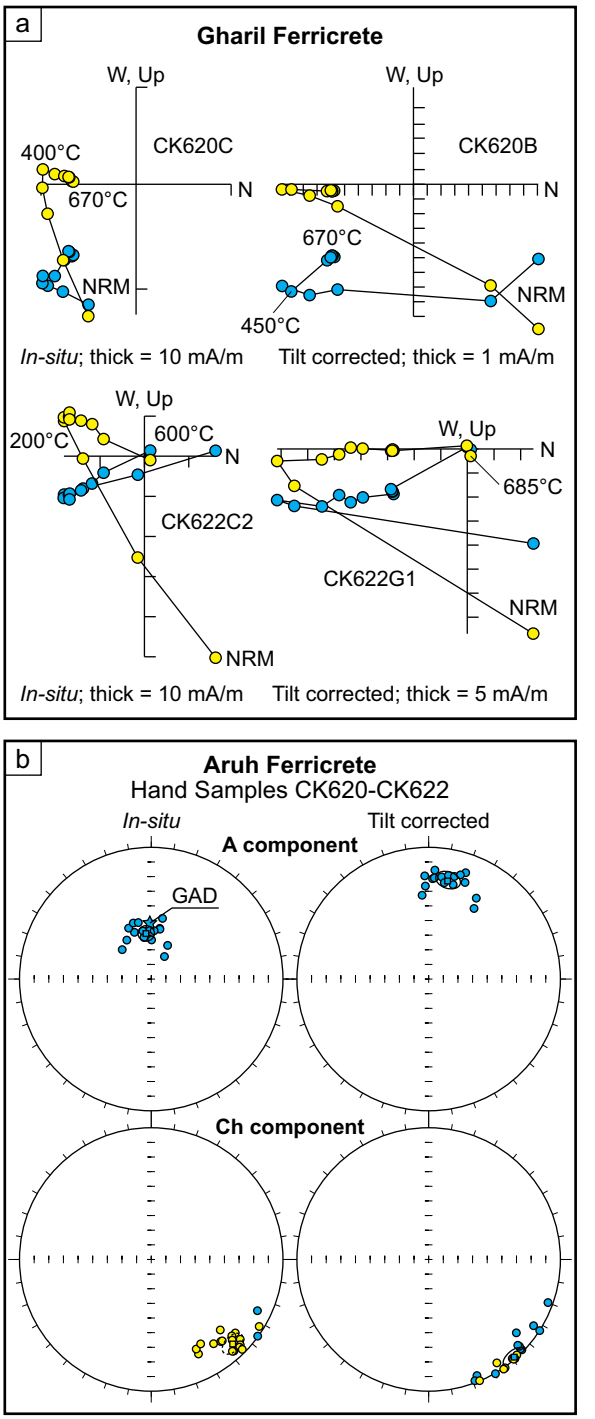

Figure 16: (a) Vector end-point demagnetization diagrams of representative samples from the Gharil ferricrete. Closed (blue) symbols are projections onto the horizontal plane and open (yellow) symbols onto the vertical plane in *in-situ* coordinates. Demagnetization temperatures are expressed in degrees centigrade ˚C. (b) Equal-area projections before (*in-situ*) and after bedding tilt correction of the characteristic component directions of the Gharil ferricrete samples. Closed (blue) symbols are projections onto the lower hemisphere and open (yellow) symbols onto the upper hemisphere. (see Table 2 for data).

Table 2
Paleomagnetic component directions from the Aruh ferricrete and the Gharil ferricrete

Comp.	T.unblock	N1/N2	R	K	α95	GDEC	GINC	R	K	α95	BDEC	BINC	Plat
Aruh ferricrete (35.66°N, 52.40°E), Upper Permian													
A	~100–250	18/08	07.9478	134.2	04.8	002.7	+52.9	07.9480	134.7	04.8	198.0	+23.7	
B	~100–325	18/04	03.9573	070.3	11.0	299.9	+81.9	03.9573	070.3	11.0	199.7	-10.4	
Ch	~350–620	18/12	11.4061	018.5	10.4	265.1	-47.8	11.4058	018.5	10.4	331.8	-01.3	-1/+1±5
Gharil ferricrete (~35.83°N, ~73.33°E), upper Middle – lower Upper Permian													
A	~030–250	21/16	15.7349	056.6	04.9	355.4	+61.5	15.6993	049.9	04.9	011.0	+25.2	
Ch	~450–670	21/19	18.4241	031.3	06.1	136.2	-12.2	18.4905	035.3	06.1	139.4	+02.7	-1/+1±3

Comp. = paleomagnetic component designation: A = (sub)recent overprint broadly consistent with the GAD direction in geographic (in-situ) coordinates, B = moderate temperature component of ancient but uncertain origin, Ch = high temperature component of presumed primary origin; T.unblock = median values of component unblocking temperatures in °C; N1/N2 = number of samples treated (N1) and number of samples that yielded stable components (N2); R = Fisher vector resultant; k, α95 = Fisher precision parameter and angle of half cone of 95% confidence about the mean direction, respectively; GDEC, GINC = mean geographic (in-situ) declination and inclination, respectively; BDEC, BINC = mean bedding (tilt corrected) declination and inclination, respectively; Plat = paleolatitude (°N when positive, °S when negative) with associated error expressed in °.

A well-defined Ch component is observed in 90% (N = 19) of the samples between median values of c. 450–670°C occasionally up to 680°C (overall MAD = 4.2° ± 3.3° SD). This Ch component is oriented southeast and moderately up in *in-situ* coordinates (Figure 16a, samples CK620C, CK622C2; Figure 16b), and southeast and very shallow upon correction for bedding tilt (Figure 16a, samples CK620B, CK622G1; Figure 16b). The tilt corrected overall mean direction (Dec. = 139.4°E, Inc. = 2.7, α95 = 5.7°; Table 2) is not compatible with any direction of Permian age expected at Gharil from the Gondwanan or Eurasian apparent polar wander path (e.g. Van der Voo, 1993; Table 2 of this study, illustrated below), and indicates a paleolatitude of c. 1° (± c. 3°) either N or S. As for the Aruh ferricrete, we regard the Ch component of the Gharil ferricrete as a pre-folding ancient magnetization acquired during lateritization processes taking place upon plate transit across equatorial paleolatitudes.

Despite the limited number of samples that yielded interpretable Ch components (N = 31 out of a total of 59 specimens analyzed), we regard these paleomagnetically determined paleolatitude estimates for ferricretes from northern Iran and the western Karakoram as highly significant whereby they quantitatively demonstrate the existence during the Permian of a climate zonality similar to that of modern-day Earth. Lateritic profiles form as a result of a weathering process, by which most of the primary minerals are dissolved and transformed into secondary minerals, chiefly haematite, goethite, Al-hydroxides (e.g. gibbsite), and kaolinite. The end-result of this process is a relative accumulation of Fe- and Al-oxides at the top of the profiles, hence the formation of duricrusts or ferricretes (Théveniaut and Freyssinet, 1999), like the Aruh and Gharil ferricretes of this study. Intensive weathering process conducive to the development of lateritic profiles and associated ferricretes occur under warm and humid conditions, which in modern-day climate are typical of the intertropical convergence zone straddling the equator (Van Houten, 1982). Our paleomagnetic analysis from the Aruh and Gharil ferricretes demonstrates that a tight connection between equatorial latitudes and the development of lateritic profiles existed also during the Permian.

The experience we developed during this reconnaissance paleomagnetic study (and that will guide our future sampling campaign, at present rescheduled due to the political turmoil in these regions of Asia) is that the rate of success in isolating stable characteristic components in laterites increases when analysis is conducted on fine-grained, homogeneous, and non-reworked ferricrete facies, as observed in several previous studies (Idnurm and Senior, 1978; Schmidt et al., 1983; Schmidt and Ollier, 1988; Acton and Kettles, 1996). To the contrary, paleomagnetic directions carried by hematite contained in micronodules (e.g. ooids, spastoliths), which can constitute distinctive accumulations also in ferricretes, can be randomly oriented due to erosion and reworking before consolidation, as observed for example in a study by Gehring et al. (1992) on ferricretes from southern Mali.

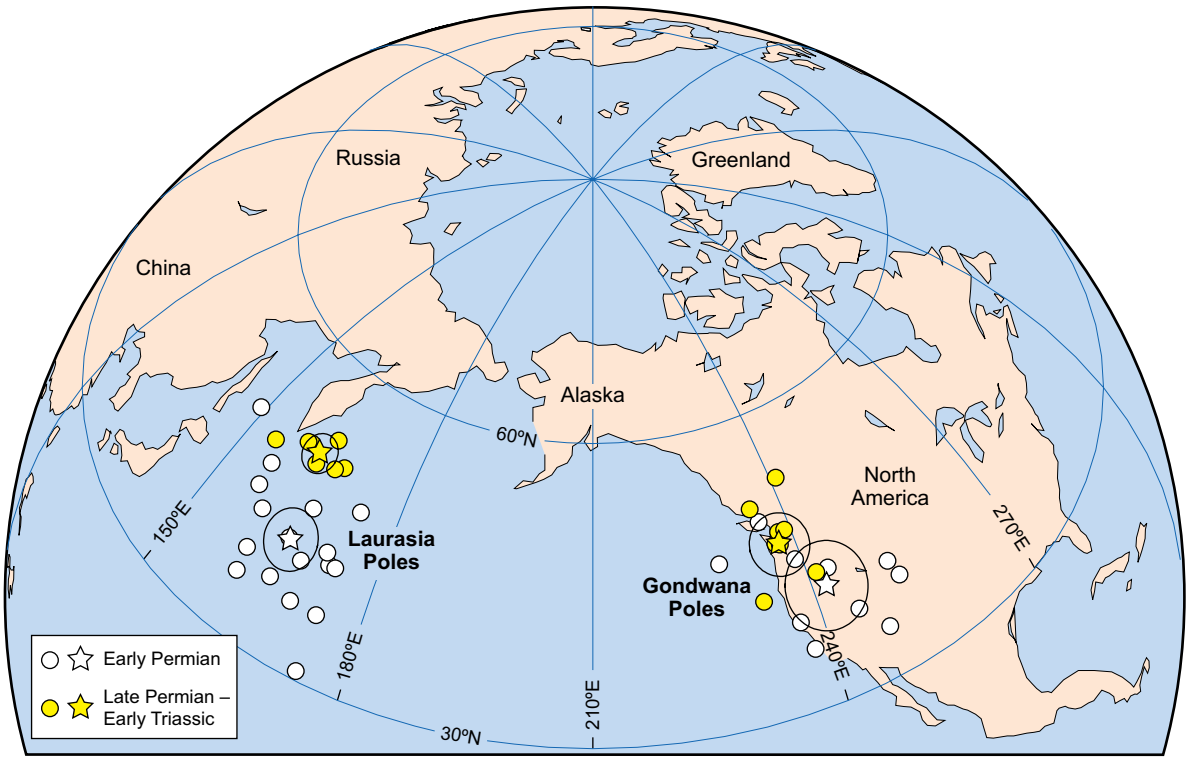

Figure 17: Early Permian and Late Permian – Early Triassic paleomagnetic poles from Gondwana and Laurasia (circles; see Table 3 for data). The Early Permian overall mean paleomagnetic pole for Gondwana (star with α95 circle of confidence) was derived from averaging paleomagnetic poles from volcanic rocks of the Southern Alps and northwest Africa dated as a whole at ca. 284–276 Ma (Muttoni et al., 2003, 2004), and the recent paleomagnetic pole of Bachtadse et al. (2002) from the Jebel Nehoud ring complex of Sudan (280 ± 2 K-Ar). The Early Permian overall mean paleomagnetic pole for Laurasia (star with α95 circle of confidence) was derived from averaging paleomagnetic poles from volcanic rocks dated as a whole at ca. 294–273 Ma (Muttoni et al., 2003, 2004). The Late Permian – Early Triassic overall mean paleomagnetic pole for Gondwana (star with α95 circle of confidence) was derived from averaging paleomagnetic poles essentially from sedimentary rocks of the Southern Alps listed in Muttoni et al. (1996). The Late Permian – Early Triassic overall mean paleomagnetic pole for Laurasia (star with α95 circle of confidence) was derived from averaging paleomagnetic poles essentially from sedimentary rocks. Middle Permian overall mean paleomagnetic poles were obtained by linear interpolation of bracketing Early Permian and Late Permian – Early Triassic overall mean poles.

PALEOGEOGRAPHY

We placed these new paleolatitude estimates for northern Iran and western Karakoram, as well as coeval paleolatitudes from the literature for adjacent Cimmerian terranes, in a set of paleomagnetic-based paleogeographic reconstructions of Pangea. In order to reconstruct the main elements of Pangea (Gondwana and Laurasia), we used a selection of paleomagnetic poles from the literature (Figure 17; Table 3) coupled with Euler poles of rotation again from the literature. Three paleogeographic reconstructions were generated, namely for the Early Permian (ca. 296–272 Ma; Figure 18), Middle Permian (ca. 272–260 Ma; Figure 19), and Late Permian – Early Triassic (ca. 260–249 Ma; Figure 20) (time scale of Menning et al., 2006).

For Gondwana, we used paleomagnetic data from Adria (AD) and NW Africa (Figure 18). Adria is considered a promontory of Africa, tectonically coherent with Northwest Africa (within paleomagnetic error resolution) since the Permian, as shown by Muttoni et al. (2003, 2004, and references therein). Both regions yielded reliable Early Permian and Late Permian – Early Triassic paleomagnetic poles (Figure 17; Table 3). Internal Gondwana plates (South America, Northeast Africa, South Africa, Greater India, Antarctica, and Australia; Figure 18) were rotated into Permian Adria-Northwest Africa coordinates using Euler poles of Lottes and Rowley (1990).

Table 3
Early Permian and Late Permian – Early Triassic paleomagnetic poles from Gondwana and Laurasia

Age	Long.	Lat.	A95	K	N	Reference
GONDWANA in NW African coordinates						
Early Permian	242.0	41.4	4.4	122	10	see *
Middle Permian (interpolated)	239.9	44.1				see $
Late Permian – Early Triassic	237.6	46.8	3.1	317	8	Muttoni et al. (1996)
LAURASIA in European coordinates						
Early Permian	166.2	42.2	3.1	126	18	Muttoni et al. (2003, Online Tab. 2)
Middle Permian (interpolated)	164.5	46.4				see $
Late Permian – Early Triassic	162.9	50.8	2.0	764	8	
calculated by averaging the following Late Permian – Early Triassic paleomagnetic poles:						
North Sudetic Sed. Zechstein	168	51	5.5			Nawrocki (1997)
Lower Buntsandstein	160	51	3			Nawrocki (1997)
Intraudetic Sed. Zechstein	166	51	3			Szurlies et al. (2003)
Buntsandstein Holy Cross	155	49	2			Nawrocki et al. (2003)
Saint-Pierre pelites	163	50	5			Diego-Orozco and Henry (1993)
Massif du Maures pelites	161	51	4			Merabet and Daly (1986)
St Affrique sediments	167	50	12			Cogne et al. (1993)
Lunner dykes 243±5 Ar/Ar	164	53	6			Torsvik et al. (1998)

Long = Longitude of paleomagnetic pole in °E; Lat. = Latitude of paleomagnetic pole in °N; A95 = estimated radius of circle of 95% confidence about the paleomagnetic pole in °; K = Fisherian precision parameter; N = number of paleomagnetic pole entries; Reference = reference to articles used in compilation (note: only references not cited in text are reported; for the other references listed in table, see paper reference list) Diego-Orozco, A., and Henry, B., 1993, Tecnophysics, v. 227, p. 31-47. Merabet, N., and Daly, L., 1986, Earth and Planetary Science Letters, v. 80, p. 156-166. Cogné, J.P., Van Den Driessche, J., and Brun, J.P., 1993, Earth and Planetary Science Letters, v. 115, p. 29-42. Torsvik, T.H., Eide, E.A., Meert, J.G., Smethurst, M.A., and Walderhaug, H.J., 1998, Geophysical Journal International, v. 135, p. 1045-1059.
** Based on N=9 paleomagnetic poles listed in Muttoni et al. (2003, online table 2) and the paleomagnetic pole from the Jebel Nehoud ring complex, Sudan (280 ± 2 K/Ar) of Bachtadse et al. (2002).*
$ Middle Permian overall mean paleomagnetic poles for Gondwana and Europe are obtained by simple interpolation of the Early Permian and Late Permian–Early Triassic overall mean paleomagnetic poles listed in table.

The paleogeography of Laurasia (North America, Europe, Siberia; Figure 18) was reconstructed adopting paleomagnetic poles from Europe (Figure 17; Table 3) assuming coalescence of Siberia and Kazhakstan with Europe (Baltica) along the Ural suture (Figure 18) essentially completed by the Permian (e.g. Matte, 2001). North America attached to Greenland (GR; Figure 18) was rotated into Permian European coordinates using Euler poles of Bullard et al. (1965). Additional Asian terranes, Junggar, Qaidam and Tarim (Figure 18) are placed in these reconstructions following Enkin et al. (1992) and Van der Voo (1993). Late Carboniferous – Triassic paleomagnetic data for Junggar and Tarim indicate paleolatitudes compatible with those predicted from Siberia (see references in Van der Voo, 1993); hence, in our Permian reconstructions, these terranes are placed close to the Eurasian margin.

Mongolia, North China, South China, and Indochina (Figure 18) were positioned following paleomagnetic and biogeographic data and reconstructions from the literature (Enkin et al., 1992; Van der Voo, 1993; Metcalfe, 2002; Torsvik and Cocks, 2004; Metcalfe, 2006; Ruban et al., 2007). In sum, paleomagnetic data for North and South China are scarce for most of the Paleozoic, and their latitudinal positions are consequently poorly established (Van der Voo, 1993). South China apparently broke off from the margin of Gondwana in the southern hemisphere during the Ordovician while North China was an isolated block in the northern hemisphere. As a consequence of their Paleozoic relative motion, North and South China collided with one another during the Permian – Triassic (Cocks and Torsvik, 2002). Late Permian paleomagnetic data for North and South China are relatively more abundant (Van der Voo, 1993) and indicate that these blocks were located at paleolatitudes spanning the equator into the tropics of the northern hemisphere (see also Enkin et al., 1992; Torsvik and Cocks, 2004). We adopt similar equatorial–northern tropical paleolatitudes also for the Early – Middle Permian. As regards Mongolia, paleomagnetic data are scarce (Van der Voo, 1993). Those of Late Permian age

EARLY PERMIAN (ca. 296–272 Ma) PANGEA B

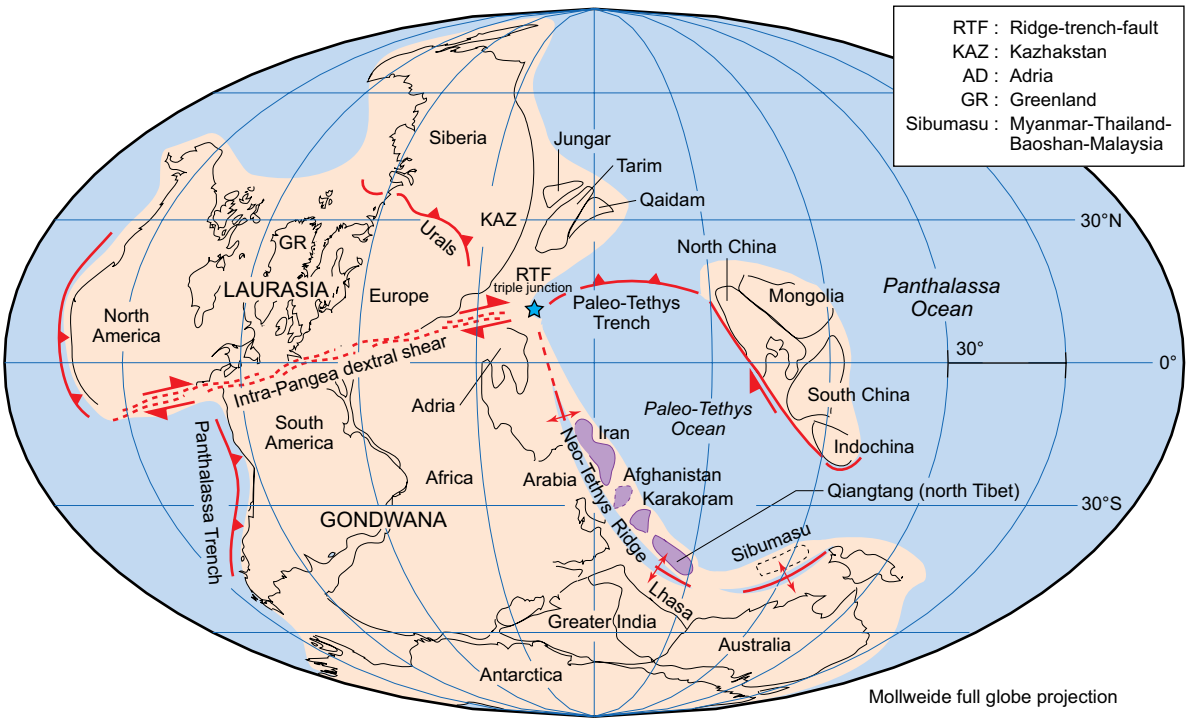

Figure 18: Paleogeographic reconstruction of Pangea B for the Early Permian based on paleomagnetic poles from Figure 17 and Table 3. The star to the northeast of Adria indicates the hypothetical location of a ridge-trench-fault (RTF) triple junction adjoining the Gondwana, Laurasia, and Paleo-Tethys plates. Plate boundaries discussed in the text are, from west to the east, the Panthalassa trench, the intra-Pangea dextral shear system, the Neo-Tethys ridge, and the Paleo-Tethys trench. Trenches are indicated by solid triangles, ridges by small diverging arrows, while half arrows indicate transcurrent plate motion. Terranes of uncertain position are represented by dashed lines (i.e. central Afghanistan, Lhasa, Sibumasu). Reconstruction made with PaleoMac (Cogné, 2003).

MIDDLE PERMIAN (ca. 272–260 Ma) PANGEA B TRANSFORMING TO PANGEA A

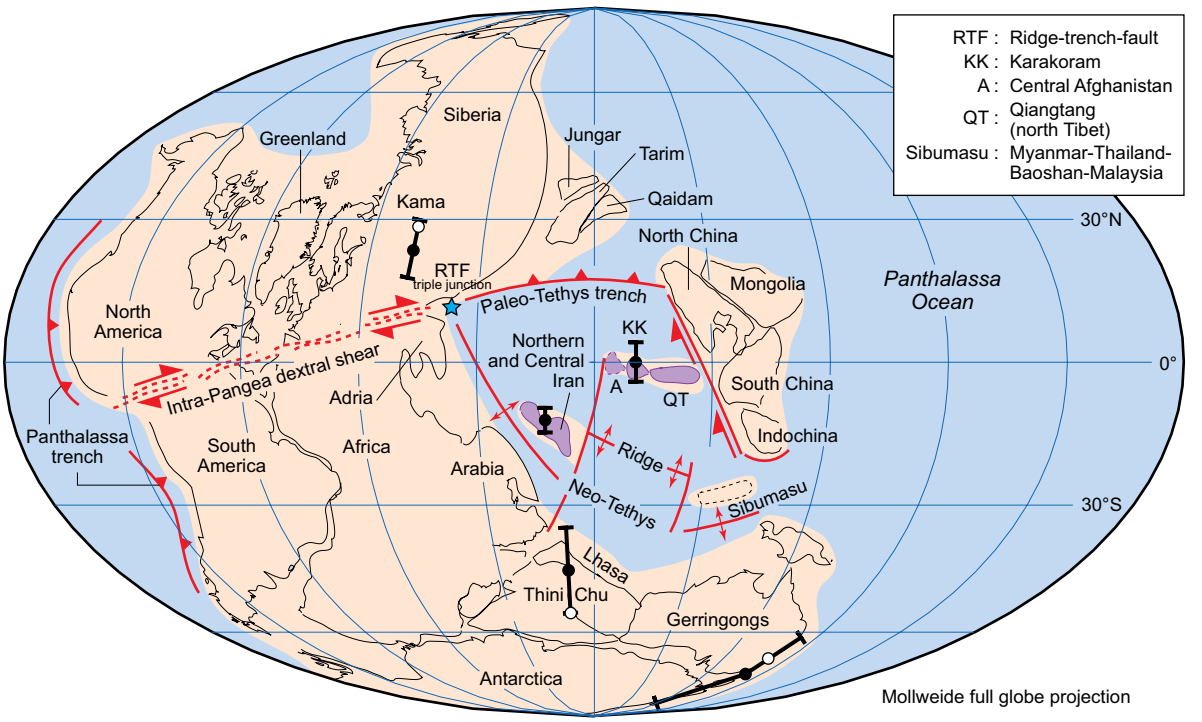

Figure 19: *(see facing page for caption)*

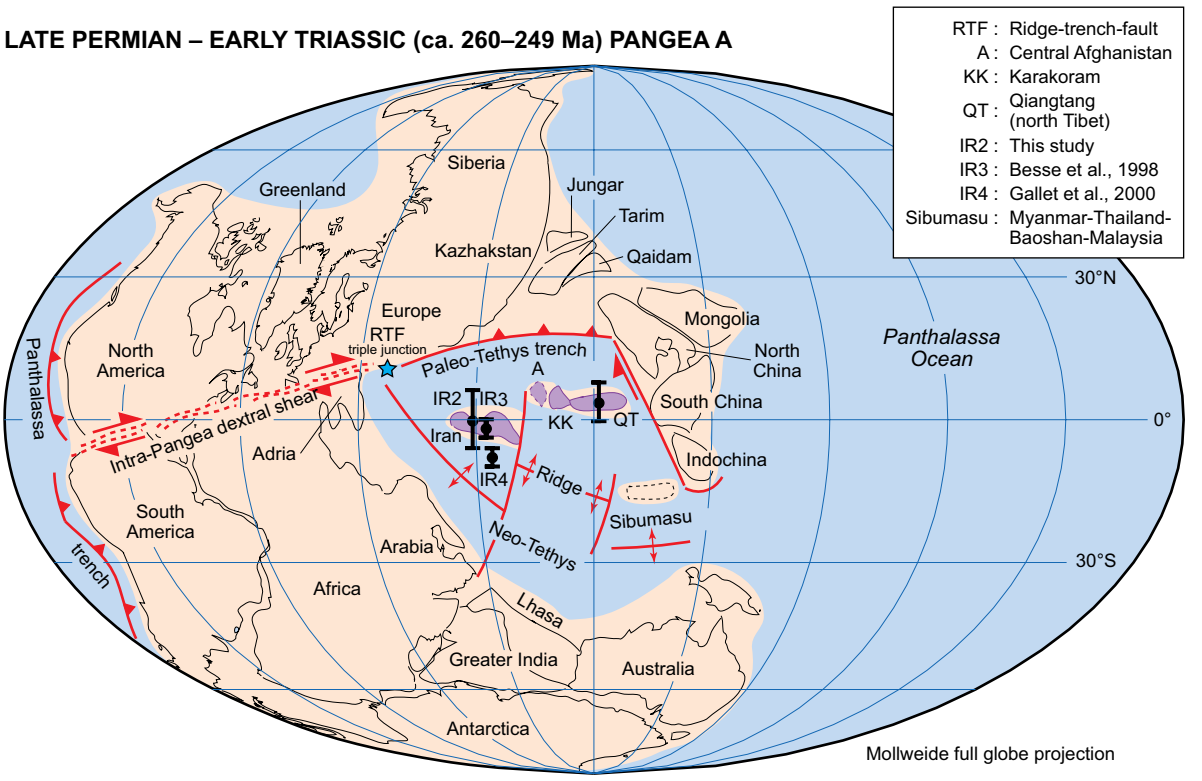

Figure 20: Paleogeographic reconstruction of Pangea A for the Late Permian – Early Triassic based on paleomagnetic poles from Figure 17 and Table 3. The star to the northeast of Adria indicates the hypothetical location of a ridge-trench-fault (RTF) triple junction adjoining the Gondwana, Laurasia, and Paleo-Tethys plates. The Paleo-Tethys and Panthalassa trenches are indicated by solid triangles, the Neo-Tethys ridge by small diverging arrows, while half arrows indicate transcurrent plate motion. Entries labeled 'IR2', 'IR3', 'IR4', and 'QT' with error bars represent the observed paleolatitudes of, respectively, the Aruh ferricrete from the Alborz region of north Iran (IR2; this study), the Hambast Formation from Abadeh in central Iran (IR3; Besse et al., 1998), the Hambast and Elikah formations from Abadeh in central Iran (IR4; Gallet et al., 2000), and the Tuoba Formation from eastern Qiangtang (QT; Huang et al., 1992). Reconstruction made with PaleoMac (Cogné, 2003).

Figure 19 *(see facing page)***: Paleogeographic reconstruction of Pangea undergoing transformation from Pangea B to Pangea A during the Early Permian; reconstruction based on paleomagnetic poles from Table 3. The star to the northeast of Adria indicates the hypothetical location of a ridge-trench-fault (RTF) triple junction adjoining the Gondwana, Laurasia, and Paleo-Tethys plates. The Paleo-Tethys and Panthalassa trenches are indicated by solid triangles, the Neo-Tethys ridge by small diverging arrows, while half arrows indicate transcurrent plate motion. Entries labeled 'IR1' and 'KK' with error bars represent the observed paleolatitudes of, respectively, the Ruteh lavas from the Alborz region of north Iran (Besse et al., 1998), and the Gharil ferricrete from the western Karakoram of this study. Entries labeled 'Kama', 'Thini Chu', and 'Gerringong' with error bars represent the observed paleolatitudes of the Kama region sediments combined (Khramov, 1982), the Thini Chu Group of Nepal (Klootwijk and Bingham, 1980), and the Gerringong volcanics (Irving and Parry, 1963); the empty circles associated with these error bars represent the paleolatitudes expected at these sites from the paleogeographic reconstruction. Reconstruction made with PaleoMac (Cogné, 2003).**

indicate subtropical northerly paleolatitudes that match the paleolatitudes predicted from the North China results; namely, Mongolia and North China were most probably adjacent at least in the Late Permian (Van der Voo, 1993). In absence of further information, we adopt a Mongolia-North China affinity also for the Early – Middle Permian. Finally, as regards Indochina, virtually all pre-Neogene paleomagnetic data are apparently remagnetized (Van der Voo, 1993). This terrane is placed close to South China in the Permian based on biogeographic data (e.g. Metcalfe, 2002; 2006).

The Cimmerian terranes of Iran (IR; Central Iran and Alborz), Karakoram (KK), and Qiangtang (QT; also known as North Tibet; Figure 18) are placed within these reconstructions using paleomagnetic data (this study; Wensink, 1979; Huang et al., 1992; Besse et al., 1998; Gallet et al., 2000) as well as geologic-biogeographic constraints, as extensively discussed in the following paragraphs. The Cimmerian Sibumasu Terrane (Myanmar-Thailand-Baoshan-Malaysia) is broadly placed within the reconstructions following mainly geologic-biogeographic arguments discussed in Metcalfe (2002; 2006). The scarcely investigated central Afghanistan Terrane (A; Figure 18) is considered a Cimmerian terrane following Sengör (1979), and tentatively placed to the east of Iran during the Permian. Finally, the position of the Tibetan Lhasa Terrane in the Permian is still a matter of debate, also for the lack of reliable paleomagnetic data (see discussion in Metcalfe, 2002). In our reconstructions, we followed Metcalfe (2002) and placed the Lhasa Terrane attached to the Gondwanan margin of India during Cimmerian motion in the Permian.

Early Permian

The Early Permian paleomagnetic poles from Gondwana (Adria-Northwest Africa) and Laurasia (Europe) (Figure 17; Table 3), coupled with the Euler poles of rotation outlined above, support a Pangea B configuration essentially similar to that originally proposed by Irving (1977) and confirmed by subsequent analyses (Morel and Irving, 1981; Muttoni et al., 1996; Torq et al., 1997; Bachtadse et al., 2002; Muttoni et al., 2003, 2004; Angiolini et al., 2007) (Figure 18). As outlined in the Introduction, however, it is fair to say that Pangea B and its tectonic implications have not been widely accepted by the earth sciences community whereby the Wegenerian Pangea A is the most widely assumed paleogeographic scenario from coalescence of Gondwana with Laurasia in the Late Paleozoic to the opening of the Atlantic Ocean in the Jurassic (ca. 300–180 Ma) (e.g. Van der Voo, 1993; Scotese, 2001; Stampfli and Borel, 2002; Ziegler et al., 2003; Torsvik and Cocks, 2004). But if the paleomagnetic poles from Gondwana and Laurasia of this study are used as a template to reconstruct a classic Wegenerian Pangea A in the Early Permian, an untenable latitudinal overlap of c. 1,000 km between Gondwana and Laurasia that involves cratonic portions of both supercontinents is produced (see figure 6 in Muttoni et al., 2003).

Two explanations have been put forward to explain such a paleolatitudinal misfit in order to maintain a Pangea A model in the Early Permian and in general from the Late Paleozoic until the Early Jurassic. According to Van der Voo and Torsvik (2001), and Torsvik and Van der Voo (2002), Pangea B is an artifact of large nondipole geomagnetic field contributions, whereas according to Rochette and Vandamme (2001), Pangea B is an artifact of inclination error in sediments. In an attempt to resolve this conundrum, Muttoni et al. (2003, 2004) used paleomagnetic data from igneous rocks from sampling sites confined to a narrow band of paleolatitudes from the same hemisphere of both Gondwana and Laurasia, thereby limiting the potential effects of inclination error, which is common in sediments but unknown to igneous rocks, as well as of zonal octupole (G3) field contributions. Under such circumstances, in fact, introducing even a c. 20% G3 component (Van der Voo and Torsvik, 2001) would simply produce a small northward displacement of both Gondwana and Laurasia while substantially maintaining the misfit in their respective paleopoles when reconstructed in a Pangea A configuration, and it is precisely such a misfit that motivated the Pangea B concept. Hence, Muttoni et al. (2003, 2004) concluded in favor of Pangea B in the Early Permian. This conclusion is reiterated here because the Early Permian paleomagnetic poles for Laurasia and Gondwana of this study (Figure 17; Table 3) coincide with those used by Muttoni et al. (2003, 2004), with the sole addition in the Gondwnan dataset of the recent paleomagnetic pole from the Jebel Nehoud ring complex of Sudan dated by K/Ar to 280 ± 2 Ma (Bachtadse et al., 2002).

Within Pangea B, the Cimmerian terranes are placed close to the Gondwanan margin in the Early Permian on the basis of geological, paleontological, and paleomagnetic evidences (Figure 18). Muttoni et al. (2009) presented new Late Ordovician paleomagnetic data and reviewed Paleozoic data from the literature from Iran. They observed a robust congruence of paleomagnetic poles of Iran and West Gondwana during the Late Ordovician – earliest Carboniferous when Gondwana experienced significant plate motion, drifting from high southern latitudes in the Late Ordovician to subequatorial latitudes in the Early Devonian and back to intermediate southern latitudes in the Late Devonian – Early Carboniferous (McElhinny et al., 2003). This is consistent with observations by several authors on the Proterozoic – Paleozoic Gondwanan ancestry of northern and central Iran based on the nature of their basement and the overlying sedimentary succession (Stöcklin, 1968; 1974; Berberian and King, 1981; Wendt et al., 2005). The Iranian terranes were therefore located close to the Arabian margin of Gondwana up to the late Paleozoic. Similar geological arguments pointing to a Paleozoic Gondwanan affinity can be drawn also for western Karakoram (e.g. Gaetani, 1997), Lhasa (whether or not it was a Cimmerian terrane) (e.g. Garzanti et al., 1999), Qiangtang and Sibumasu (e.g. Shi et al., 1995; Metcalfe, 2002; 2006).

Neo-Tethyan rifting along the eastern Gondwana margin started in Carboniferous time from India (Garzanti and Sciunnach, 1997) to Oman (Al-Belushi et al., 1996). In northwestern Himalaya, Neo-Tethyan rifting reached its climax with the onset of bimodal volcanism and intrusion of alkali granites, dated at 284 ± 1 Ma (U-Pb on zircons; Spring et al., 1993) and biostratigraphically constrained to the earliest Permian (Garzanti et al., 1996). Continental break-up and formation of oceanic lithosphere followed shortly afterwards from the Himalayas all the way to northern Oman in the mid-Early Permian (mid-Sakmarian; Garzanti, 1999; Angiolini et al., 2003a). Shi et al. (1995), Shi and Archbold (1998), and Metcalfe (2006) proposed a substantially similar (late Sakmarian) timing of formation of Neo-Tethyan oceanic lithosphere between the Indo-Australian margin and the Qiangtang and Sibumasu terranes. Hence, the separation from Gondwana of the Cimmerian terranes, previously attached to the Arabia-Australia margin from Iran to Sibumasu via western Karakoram and Qiangtang, initiated with Neo-Tethyan spreading approximately during the middle part of the Early Permian, or ca. 290–284 Ma (time scale of Menning, 2006) (Figure 18).

At approximately the same time, a major zone of northward subduction of Paleo-Tethyan oceanic lithosphere was activated along the southern Eurasian margin and persisted during most of the Permian – Triassic (e.g. Alavi, 1991; Ruttner, 1993; Dercourt et al., 1993; Alavi, 1996; Alavi et al., 1997; Besse et al., 1998; Metcalfe, 2006; Shi, 2006; Zanchi et al., 2009a; 2009b). Some authors (e.g. Sengör, 1979) argued for a southward subduction of Paleo-Tethyan oceanic lithosphere under the Cimmerian terranes during the opening of the Neo-Tethys (back-arc) Ocean. We believe, however, that the most convincing geologic evidence for Paleo-Tethys subduction such as calcalkaline magmatism, strong regional deformation, and metamorphism are jointly present along the southern portion of the Eurasian Plate, for example in southern Turan (Eurasia) and northern Iran (Alavi, 1991, 1996; Ruttner, 1993; Alavi et al., 1997; Zanchi et al., 2009a, b).

To the west along the former Variscan Suture of Europe, a zone of diffused dextral shear lubricated by abundant magmatism started to develop between Gondwana and Laurasia (Muttoni et al., 2003, 2004; and references therein). For example, in the Southern Alps of Italy (northern part of Adria; AD in Figure 18), dextral pull-apart basins associated with magmatism formed during a short time span between 285 and 275 Ma (Schaltegger and Brack, 2007). The silicic magmatism is coeval with mafic intrusions of the Ivrea-Verbano Zone and within Austroalpine units. Deep magma generation, hybridisation and upper crustal emplacement occurred contemporaneously along the entire transect of the Southern Alps (Schaltegger and Brack, 2007). As we shall see in the next section, these Permian intra-continental basins, well studied in the Southern Alps but known also from NW Africa and across much of central Europe, formed and evolved during large-scale, strike-slip tectonics that may correspond to the transformation from Early Permian Pangea B to Late Permian Pangea A (Muttoni et al., 2003, 2004; Schaltegger and Brack, 2007).

Three major plates, i.e. Gondwana, Laurasia, and Paleo-Tethys (including the Cimmerian terranes) seemed to have existed in the Early Permian. The Gondwana plate was bounded to the east by the Neo-Tethyan ridge, to the west by the Panthalassan trench of South America, and to the north by

the intra-Pangea dextral shear system forming a diffuse margin with Laurasia (Figure 18). Laurasia was bounded to the west by the Panthalassan trench of North America and to the south by the afore-mentioned dextral shear system, which farther east was substituted by the trench marking the subduction of the Paleo-Tethyan oceanic lithosphere (Figure 18). The Paleo-Tethys Plate was bounded to the west by the Neo-Tethyan ridge, to the north by the Paleo-Tethyan trench, and to the east by a transform margin supposedly located along the western side of the China blocks (Enkin et al., 1992; Metcalfe, 2006) (Figure 18). The Paleo-Tethys Plate was composed of Paleo-Tethyan oceanic lithosphere and of a set of Cimmerian terranes (e.g. Iran, Afghanistan, Karakoram, Qiangtang) separated by transform faults displacing the Neo-Tethyan ridge (e.g. ancestral Hari Rud Fault between Iran and Afghanistan; Wellman, 1965; Boulin, 1991). The Gondwana, Laurasia, and Paleo-Tethys plates were joined at a ridge-trench-transform fault (RTF) triple junction presumably located somewhere to the northeast of Adria (star in Figure 18). Notably, RTF triple junctions of the type presently observed at the southern end of the Gulf of California, are considered stable and long lasting in case of alignment of the intervening transform and trench margins (McKenzie and Morgan, 1969). This is a realistic possibility in our reconstruction whereby the intra-Pangea dextral shear system and the Panthalassan trench were broadly aligned along the same great circle transect (Figure 18).

Middle Permian

The Middle Permian paleogeographic reconstruction is based on a linear interpolation of bracketing Early Permian and Late Permian – Early Triassic paleomagnetic poles from Gondwana (Adria-Northwest Africa) and Laurasia (Europe). It shows Pangea undergoing transformation from an Irvingian B to a Wegenerian A geometry by way of the intra-Pangea dextral shear system between Gondwana and Laurasia outlined in the previous section (Figure 19). In order to test the validity of this interpolated reconstruction, we selected paleomagnetic data of Middle Permian age from various continents from the literature and used them as latitude checkpoints. These are paleolatitude estimates for the Kama region sediments combined (Khramov, 1982), the Middle Permian part of the Thini Chu Group of Nepal (Klootwijk and Bingham, 1980), and the Gerringong volcanics of Australia (Irving and Parry, 1963). Inspection of Figure 19 reveals that the Kama, Thini Chu, and Gerringong direct estimates of paleolatitude are broadly compatible with the estimates predicted at the individual sites by our Middle Permian paleogeographic reconstruction (Figure 19, open circles).

Within this Pangea configuration, we placed the paleolatitude estimate obtained by Besse et al. (1998) (see also Wensink, 1979) for the Ruteh lavas from central Alborz (northern Iran). These lavas are interbedded within Capitanian (late Middle Permian) sediments of the Ruteh Formation and are unambiguously older than the Late Permian Aruh lateritic profile (Figure 8, lower part of Bear Gully section; Gaetani et al., 2009) that paleomagnetic analysis showed to have formed at equatorial paleolatitudes. The notion that Iran had Arabian affinity in the Paleozoic, detached from Arabia by Neo-Tethyan spreading in the mid-Early Permian, and attained equatorial paleolatitudes by the Late Permian (Aruh lateritic profile) is used to interpret the hemisphere of magnetization acquisition of the Ruteh lavas, the polarity of which is unknown.

The simplest scenario is to place the Alborz region, within which the Ruteh lavas are located, at a paleolatitude of c. 12°S ± 2° to the north of the Arabian margin in the late Middle Permian (IR1 in Figure 19), in agreement with the original interpretation of Besse et al. (1998). Farther to the east in the Neo-Tethys Ocean, the Gharil ferricrete of this study formed as the western Karakoram Terrane was stationed at equatorial paleolatitudes of c. 1°S/1°N ± 3° during middle – late Middle Permian time (KK in Figure 19). Hence, the northward drift of the Cimmerian terranes was well on its way during the Middle Permian. Acknowledging the possibility that the equatorial Gharil ferricrete may not be synchronous with the low southern latitude Ruteh lavas, we speculate that the Neo-Tethys Ocean opened asymmetrically with higher seafloor spreading rates for the central Cimmerian terranes (central Afghanistan, western Karakoram, and Qiangtang) than for western terranes such as Iran, possibly due to a transform margin dissecting the Neo-Tethyan ridge between Iran and western Karakoram (Figure 19).

Middle Permian differential drift of Cimmerian terranes including Sibumasu is supported by paleobiogeographic affinities of brachiopod faunas. Middle Permian (Wordian) brachiopods from the Alborz Mountains of northern Iran contain a significant proportion of Gondwanan taxa, some of which are restricted to the Gondwanan margin (Oman and Turkey; Angiolini et al., 2003b) or to the southeastern Cimmerian terranes (Sibumasu). Middle Permian (Roadian – Wordian) brachiopods from central Afghanistan and Karakoram are remarkably different from those from both Iran and Peri-Gondwana and were interpreted as pertaining to a separate, low-latitude bioprovince (Angiolini, 2001). Middle Permian faunas from southern Thailand and the western belt of Malaysia, both considered part of the Sibumasu Terrane, show affinity with Peri-Gondwanan faunas of Oman and the Salt Range of Pakistan (Angiolini, 2001; Campi et al., 2005). Hence, paleobiogeographic data suggest that the central Cimmerian terranes (e.g. central Afghanistan, Karakoram) were displaced northward with respect to the western (Iran) and eastern (Sibumasu) terranes, an observation that agrees substantially with the available paleomagnetic data.

The Middle Permian reconstruction depicts an internally consistent Gondwana–Laurasia–Paleo-Tethys plate circuit that does not apparently violate viable plate boundary geometries and visual mass balance estimates of lithosphere emplaced at spreading ridges and consumed at subduction trenches. In short, new oceanic lithosphere emplaced at the Neo-Tethyan ridge was in part accommodated by the synchronous subduction of old Paleo-Tethys oceanic lithosphere at the Paleo-Tethyan trench, which was active during most of the Permian – Triassic (e.g. Dercourt et al., 1993; Besse et al., 1998; Alavi et al., 1997; Metcalfe, 2006; Shi, 2006). The remainder of the Neo-Tethyan oceanic lithosphere was accommodated by the dextral transcurrent motion of Laurasia relative to Gondwana along the intra-Pangea shear system. The motion of Laurasia relative to Gondwana was in turn accomodated by the subduction of Panthalassan oceanic lithosphere along the west side of the Americas (Figure 19). The RTF triple junction where the Gondwana, Laurasia, and Paleo-Tethys plates joined (star in Figure 19) remained presumably stable over the Middle Permian because the intra-Pangea dextral shear system and the Panthalassan trench were broadly aligned along the same great circle transect (Figure 19).

The timing of these plate tectonic events can be best estimated using geologic and stratigraphic data from the Southern Alps of Italy (northern part of Adria; Figure 18). In the transtensional basins that formed along the entire transect of the Southern Alps during the Early Permian (285–275 Ma), magmatism and clastic sedimentation were interrupted at 275 Ma and for the ensuing 10–15 million years (Schaltegger and Brack, 2007). Such a Middle Permian unconformity, recognized also elsewhere in Permian basins of central Europe, may have originated during large-scale strike-slip tectonics and erosion that was associated with crustal thinning, upwelling and partial melting of mantle, and advection of melts and heat into the crust (Schaltegger and Brack, 2007; Froitzheim et al., 2008). The timing and duration of this continental-scale Middle Permian unconformity indeed correspond to the timing and duration of the transformation from Early Permian Pangea B to Late Permian Pangea A as proposed by Muttoni et al. (2003, 2004; see also Schaltegger and Brack, 2007).

Late Permian – Early Triassic

Late Permian – Early Triassic paleomagnetic poles from Gondwana (Adria-Northwest Africa) and Laurasia (Europe), discussed previously, indicate that the transformation from Pangea B to Pangea A-type was completed by that time (see also Muttoni et al., 2003, 2004) (Figure 20). Within this Pangea A-type reconstruction, we placed the new data from the Aruh ferricrete that suggest equatorial paleolatitudes of c. 1°S to 1°N ± 5° for the Alborz area of northern Iran in the Late Permian (IR2 in Figure 20). Subequatorial paleolatitudes were also determined for the Late Permian Hambast Formation by Besse et al. (1998) (site IR3) and the Late Permian – Induan Hambast and Elikah formations by Gallet et al. (2000) (site IR4) from Abadeh in central Iran. Here, the polarity of magnetization is known from magnetostratigraphic correlations with sections from the literature of believed known sense of polarity. The sampled units were located at paleolatitudes of c. 2°S ± 2° for site IR3 and at a somewhat higher paleolatitude of c. 8°S ± 1.5° for site IR4 (Figure 20).

Farther to the east in the Neo-Tethys Ocean, Huang et al. (1992) found subequatorial paleolatitudes (c. 3°N ± 4°) in the Late Permian Tuoba Formation from the eastern Qiangtang Terrane (QT in Figure 20), paleogeographically located to the east of the western Karakoram Terrane. As pointed out by Huang et al. (1992), these equatorial paleolatitudes and the similarity of Late Permian fauna and flora shared by Qiangtang Terrane and the South China Block (Figure 20) suggest that the two terranes were in close proximity during the Late Permian. Therefore, we suggest that northern Iran (Alborz), Central Iran (Abadeh), the Qiangtang Terrane, and possibly also the intervening Afghanistan and Karakoram terranes, resided at subequatorial paleolatitudes in Late Permian – Early Triassic times (Figure 20). In the east, the Sibumasu Terrane, after late Sakmarian (mid Early Permian) separation from Gondwana, approached the China blocks in the Late Permian, as testified by the marine provinciality of its fauna, which turned from an essentially Gondwanan-type in the Early – Middle Permian to a warm-temperate mixed Gondwanan – Cathaysian one in the Late Permian (Shi et al., 1995; Shi and Archbold, 1998).

DISCUSSION AND CONCLUSIONS

We obtained new paleomagnetic data from northern Iran and western Karakoram (Pakistan) on fine-grained and homogeneous ferricretes preserved in lateritic profiles, where long-term lateritization processes were responsible for the acquisition of stable low-inclination chemical remanent magnetizations carried essentially by hematite. This is in line with previous studies from, for example, peninsular India and Australia that showed the reliance of fine-grained, homogeneous, and non reworked laterites as reliable recorders of consistent paleomagnetic directions (Idnurm and Senior, 1978; Schmidt et al., 1983; Schmidt and Ollier, 1988; Acton and Kettles, 1996), and in opposition to studies on micronodule-rich ferricrete facies that were shown to carry randomly distributed paleomagnetic directions due to reworking before consolidation of the ferricretes (Gehring et al., 1992). The lateritic profiles of this study originated at equatorial paleolatitudes, as demonstrated by the characteristic paleomagnetic component retrieved from the ferricretes. Because lateritic profiles develop as a consequence of intensive weathering processes under warm and humid conditions, our paleomagnetic analysis demonstrates the existence in the Permian of a tight coupling between equatorial latitudes and warm-humid climate conductive to lateritization, which is reminiscent of modern-day Earth's climate zonality.

We used paleomagnetic data from the literature from Gondwana and Laurasia to generate a set of paleogeographic reconstructions for Pangea during the Permian. The Early Permian paleomagnetic poles from Gondwana and Laurasia support a Pangea B configuration essentially similar to that originally proposed by Irving (1977), whereas Late Permian – Early Triassic poles support a classic Wegenerian Pangea A. Therefore, Pangea seemingly evolved from an Irvingian B to a Wegenerian A-type configuration during the Permian, as proposed by Muttoni et al. (2003, 2004). Within this evolving Pangea, we placed our new paleomagnetic estimates of paleolatitude from northern Iran and western Karakoram, in conjunction with data from the literature from Iran and Qiangtang, to investigate the relationships between Neo-Tethys Ocean opening, Cimmerian terranes motion, and Pangea evolution during the Permian (Figures 18 to 20). Acknowledging the limitations of our relatively meager paleomagnetic dataset from the Cimmerian terranes, we suggest that the western Cimmerian terranes of Iran, Karakoram, and Qiangtang migrated from southern Gondwanan paleolatitudes in the Early Permian to subequatorial paleolatitudes by the ca. Middle Permian – Early Triassic as a consequence of Neo-Tethys Ocean opening. These findings refine the timing of Cimmerian motion proposed by Sengör (1979) that was initially tested paleomagnetically by data essentially from Iran (see discussion and references in Van der Voo, 1993 and Besse et al., 1998).

One of the main outcomes of our analysis is that the Neo-Tethys Ocean may have opened asymmetrically during the Permian. In fact, terranes in the middle part of Cimmeria (e.g. western Karakoram, central Afghanistan, and Qiangtang) appear to have moved much faster in the Middle Permian and then slowed down significantly in the Late Permian – Early Triassic, whereas Iran (and possibly also Sibumasu) did not seem to have moved much in the Middle Permian relative to its large displacement in the Late Permian – Early Triassic. This is in contrast to classic reconstructions from the literature (e.g. Sengör, 1979 and Stampfli and Borel, 2002) where Cimmeria is depicted as a string of terranes ('ribbon continent') being swept away by the Neo-Tethys Ocean like a 'windscreen wiper',

opening at drift rates more or less linearly graded along the line of the moving string, i.e. slower at the proximate point in the western Tethys and faster at the more distant end in the eastern Tethys (e.g. see figure 6 in Stampfli and Borel, 2002).

In terms of continental drift and plate tectonics (Figure 18 to 20), three major plates – Gondwana, Laurasia, and Paleo-Tethys – seemed to have moved in spatio-temporal contiguity, altogether constituting an internally consistent scenario of Neo-Tethys Ocean opening, Cimmerian terranes northward drift, and Pangea B to Pangea A transformation over the course of the Permian. The Gondwana Plate was bounded to the east by the Neo-Tethyan ridge, to the west by the Panthalassan trench, and to the north by the intra-Pangea dextral shear system forming a diffuse margin with Laurasia. The Laurasia Plate was bounded to the south by the intra-Pangea shear system and by the trench marking the subduction of the Paleo-Tethyan oceanic lithosphere, and to the west by the Panthalassan trench. The Paleo-Tethys Plate was bounded to the west by the Neo-Tethyan ridge, to the north by the Paleo-Tethys trench, and to the east by a transform margin supposedly located along the western side of the China blocks. The Paleo-Tethys Plate contained a set of Cimmerian terranes (e.g. Iran, Karakoram, Qiangtang) separated by transform faults displacing the Neo-Tethyan ridge. The Gondwana, Laurasia, and Paleo-Tethys plates were joined at a ridge-trench-transform triple junction made stable and long lasting over the course of the Permian by a substantial alignment of the intervening transform and trench margins (McKenzie and Morgan, 1969).

Relative plate speeds within this evolving Permian tectonic circuit are difficult to evaluate precisely. Assuming transformation from Pangea B to Pangea A-type over a ca. 30 million year (My) interval (e.g. from ca. 280 Ma in the Early Permian to ca. 250 Ma at the ca. Permian – Triassic boundary), the dextral displacement of 3,000 km between Laurasia and Gondwana should have occurred at a relative speed of c. 10 cm/yr. Allowing a shorter duration for the transformation (ca. 20 My) would yield higher relative plate speeds up to c. 15 cm/yr (Muttoni et al., 2003, 2004). Despite the large uncertainties associated with such estimates, we stress that the amount and timing of Pangea's transformation is within the same range of values applicable to the northward motion of the Cimmerian terranes, on the order of c. 7–10 cm/yr over a ca. 30–20 My interval for Iran (see also Muttoni et al., 2009), and c. 12–17 cm/yr over a ca. 30–20 My interval for Karakoram and Qiangtang. Such plate motion speeds, albeit high, are not unusual even for plates containing a substantial fraction of continental lithosphere (Meert et al., 1993).

Conscious that the conclusions reached in this study are based on a limited set of data and observations from Cimmeria, we nevertheless suggest that the timing, rates, and geometry of Cimmerian tectonics are broadly compatible with the transformation of Pangea from an Irvingian B to a Wegenerian A-type configuration essentially in the Permian as opposed to a more orthodox view of Pangea A existing from coalescence of Gondwana with Laurasia in the Late Paleozoic to the opening of the Atlantic Ocean in the Jurassic (e.g. Van der Voo, 1993; Scotese, 2001; Stampfli and Borel, 2002; Ziegler et al., 2003; Torsvik and Cocks, 2004). We believe that the timing and rates of relative motion of Cimmerian terranes thus provide indirect evidence for the existence of Pangea B. The body of paleomagnetic evidence supportive of Pangea B and its transformation into Pangea A has been developed independently (Irving, 1977; Morel and Irving, 1981; Muttoni et al., 1996; Torq et al., 1997; Bachtadse et al., 2002; Muttoni et al., 2003, 2004; Angiolini et al., 2007) from the body of paleomagnetic evidence supportive of the northward motion of the Cimmerian terranes outlined in this study. Yet, the two datasets and the stories they convey seem to be very much complementary when linked together in a common plate tectonics scenario of Neo-Tethyan opening and Pangea transformation taking place contemporaneously essentially during the Permian.

ACKNOWLEDGMENTS

We thank the Editor Moujahed Al-Husseini and three anonymous Reviewers for critical but constructive reviews of the manuscript. A. Rizzi (CNR-IDPA, Milano) performed SEM-EDS microanalyses on the Gharil Formation. Financial support by Middle East Basin Evolution (MEBE) programme. This is Lamont–Doherty contribution #7239. GeoArabia's Arnold Egdane is thanked for designing the paper.

REFERENCES

Acton, G.D. and W.A. Kettles 1996. Geologic and palaeomagnetic constraints on the formation of weathered profiles near Invernell, eastern Australia. Palaeogeography Palaeoclimatology Palaeoecology, v. 126, no. 3-4, p. 211-225.

Al-Belushi, J.D., K.W. Glennie and B.P.J. Williams 1996. Permo-Carboniferous glaciogenic Al Khlata Formation, Oman: A new hypothesis for origin of its glaciation. GeoArabia, v. 1, no. 3, p. 389-404.

Alavi, M. 1991. Sedimentary and structural characteristics of the Paleo-Tethys remnants in northeastern Iran. American Association of Petroleum Geologists Bulletin, v. 103, no. 8, p. 983-992.

Alavi, M. 1996. Tectonostratigraphic synthesis and structural style of the Alborz Mountain system in Iran. Journal of Geodynamics, v. 21, no. 1, p. 1-33.

Alavi, M., H. Vaziri, K. Seyed Enami, and Y. Lasemi 1997. The Triassic and associated rocks of the Nakhlak and Aghdarband areas in central and northeastern Iran as remnants of the southern Turanian active continental margin. American Association of Petroleum Geologists Bulletin, v. 109, no. 12, p. 1563-1575.

Allen, M.B., M.R. Ghassemi, M. Shahrabi and M. Qorashib 2003. Accommodation of late Cenozoic oblique shortening in the Alborz range, northern Iran. Journal of Structural Geology, v. 25, no. 5, p. 659-672.

Altiner, D., A. Baud, J. Guex and G. Stampfli 1980. La limite Permien-Trias dans quelques localités du Moyen-Orient: Recherches stratigraphiques et micropaléontologiques. Rivista Italiana de Paleontologia e Stratigrafia, v. 85, no. 3-4, p. 683-714.

Angiolini, L. 2001. Lower and Middle Permian brachiopods from Oman and Peri-Gondwanan palaeogeographical reconstructions. In C.H.C. Brunton, L.R.M. Cocks and S.L. Long (Eds.), Brachiopods Past and Present. The Systematics Association Special Volume Series, v. 63, p. 352-362.

Angiolini, L., M. Balini, E. Garzanti, A. Nicora and A. Tintori 2003a. Gondwanan deglaciation and opening of Neo-Tethys: The Al-Khlata and Saiwan formations of Interior Oman. Palaeogeography Palaeoclimatology, Palaeoecology, v. 196, no. 1-2, p. 99-123.

Angiolini, L., M. Balini, E. Garzanti, A. Nicora, A. Tintori, S. Crasquin-Soleau and G. Muttoni 2003b. Permian climatic and palaeogeographic changes in northern Gondwana: The Khuff Formation of Interior Oman. Palaeogeography, Palaeoclimatology, Palaeoecology, v. 191, no. 3-4, p. 269-300.

Angiolini, L., M. Gaetani, G. Muttoni, M.H. Stephenson and A. Zanchi 2007. Tethyan oceanic currents and climate gradients 300 my ago. Geology, v. 35, no. 12, p. 1071-1074.

Assereto, R. 1963. The Paleozoic formations in central Elburz (Iran): Preliminary note. Rivista Italiana Palaeontologica e Stratigrafica, v. 69, p. 503-543.

Bachtadse, V., R. Zanglein, J. Tait and H. Soffel 2002. Palaeomagnetism of the Permo/Carboniferous (280 Ma) Jebel Nehoud ring complex, Kordofan, Central Sudan. Journal of African Earth Sciences, v. 35, no. 1, p. 89-97.

Battacharaya, D.B. 1983. Origin of berthierine in ironstones. Clays and Clay Minerals, v. 31, no. 3, p. 173-182.

Berberian, M. and G.C.P. King 1981. Towards a palaeogeography and tectonic evolution of Iran. Canadian Journal of Earth Sciences, v. 18, no. 2, p. 210-265.

Besse, J., F. Torcq, Y. Gallet, L.E. Ricou, L. Krystyn and A. Saidi 1998. Late Permian to Late Triassic palaeomagnetic data from Iran: Constraints on the migration of the Iranian block through the Tethyan Ocean and initial destruction of Pangaea. Geophysical Journal International, v. 135, no. 1, p. 77-92.

Boulin, J, 1991. Structures in southwest Asia and evolution of the eastern Tethys. Tectonophysics, v. 196, no. 3-4, p. 211-268.

Bullard, E.C., J.E. Everett and A.G. Smith 1965. A symposium on continental drift. IV. The fit of the continents around the Atlantic. Philosophical Transactions of the Royal Society of London, v. A258, p. 41–51.

Campi, M.J., G.R. Shi and M.S. Leman 2005. Guadalupian (Middle Permian) brachiopods from Sungai Toh, a Leptodus Shale locality in the central belt of Pensinsular Malalysia. Palaeontographica (A), v. 273, p. 97–160.

Cocks, L.R.M. and T.H. Torsvik 2002. Earth geography from 500 to 400 million years ago: Faunal and paleomagnetic review. Journal of the Geological Society of London. v. 159, p. 631-644.

Cogné, J.P. 2003. PaleoMac: A MacintoshTM application for treating paleomagnetic data and making plate reconstructions. Geochemistry, Geophysics, and Geosystems, v. 4, no. 1, p. 1007.

Dercourt, J., L.E. Ricou and B. Vrielynck 1993. Atlas Tethys, Palaeoenvironmental Maps. Gauthier-Villars, Paris, 307 p.

Enkin, R.J., Z. Yang, Y. Chen and V. Courtillot 1992. Paleomagnetic constraints on the geodynamic history of the major blocks of China from the Permian to the present. Journal of Geophysical Research, v. 97, no. B10, p. 13953-13989.

Froitzheim, N., J.F. Derks, J.M. Walter and D. Sciunnach 2008. Evolution of an Early Permian extensional detachment fault from synintrusive, mylonitic flow to brittle faulting (Grassi Detachment Fault, Orobic Anticline, southern Alps, Italy). Geological Society of London, Special Publication, v. 298, p. 69–82.

Gaetani, M., L. Angiolini, E. Garzanti, F. Jadoul, E. Leven, A. Nicora and D. Sciunnach 1995. Permian stratigraphy in the northern Karakorum (Pakistan). Rivista Italiana di Paleontologia e Stratigrafia, v. 101, no. 2, p. 107-152.

Gaetani, M., P. Le Fort, S. Tanoli, L. Angiolini, A. Nicora, D. Sciunnach and A. Khan 1996. Reconnaissance geology in Upper Chitral, Baroghil and Karambar districts (northern Karakorum, Pakistan). Geologishe Rundschau, Berlino, v. 85, p. 638-704.

Gaetani, M. 1997. The Karakorum block in central Asia, from Ordovician to Cretaceous. Sedimentary Geology, v. 109, no. 3, p. 339-359.

Gaetani, M., A. Zanchi, L. Angiolini, G. Olivini, D. Sciunnach, H. Brunton, A. Nicora and R. Mawson 2004. The Carboniferous of the Western Karakorum (Pakistan). Journal of Asian Earth Science, v. 23, no. 2, p. 275-305.

Gaetani, M., L. Angiolini, K. Ueno, A. Nicora, M. Stephenson, D. Sciunnach, R. Rettori, G. Price and J. Sabouri 2009. Pennsylvanian to Early Triassic stratigraphy in the Alborz Mountains (Iran). In M.-F. Brunet, M. Wilmsen and J.W. Granath (Eds.), South Caspian to Central Iran Basins. Geological Society of London Special Publication no. 312, in press.

Gallet, Y., L. Krystyn, J. Besse, A. Saidi and L.-E. Ricou 2000. New constraints on the Upper Permian and Lower Triassic geomagnetic polarity timescale from the Abadeh section (central Iran). Journal of Geophysical Research, v. 105, no. B2, p. 2805-2815.

Garzanti, E., L. Angiolini and D. Sciunnach 1996. The mid–Carboniferous to lowermost Permian succession of Spiti (Po Group and Ganmachidam Formation; Tethys Himalaya, Northern India): Gondwana glaciation and rifting of Neo-Tethys. Geodinamica Acta, v. 9, no. 2, p. 78-100.

Garzanti, E. and D. Sciunnach 1997. Early Carboniferous onset of Gondwanian glaciation and Neo-Tethyan rifting in southern Tibet. Earth Planetary Science Letters, v. 148, no. 1, p. 359-365.

Garzanti, E. 1999. Stratigraphy and sedimentary history of the Nepal Tethys Himalayan passive margin. In B.N. Upreti and P. Le Fort (Eds.), Advances on the Geology of the Himalaya - Focus on Nepal. Journal of Asian Earth Sciences, v. 17, no. 5, p. 805-827.

Garzanti, E., P. Le Fort and D. Sciunnach 1999. First report of Lower Permian basalts in South Tibet: Tholeiitic magmatism during break-up and incipient opening of Neo-Tethys. Journal of Asian Earth Sciences, v. 17, no. 4, p. 533-546.

Gehring, A.U., P. Keller and F. Heller 1992. Magnetic evidence for the origin of lateritic duricrusts in southern Mali (Western Africa). Palaeogeography, Palaeoclimatology, Palaeoecology, v. 95, no. 1-2, p. 33-40.

Glaus, M. 1964. Trias und oberperm in Zentralen Elburz (Persien). Eclogae Geologicae Helveticae, v. 57, no. 2, p. 497-508.

Hayden, H.H. 1915. Notes on the geology of Chitral, Gilgit and the Pamirs. Records of the Geological Survey of India, v. 45, p. 271-320.

Huang, K., N.D. Opdyke, X. Peng and J. Li 1992. Paleomagnetic results from the Upper Permian of the eastern Qiangtang Terrane of Tibet and their tectonic implications. Earth and Planetary Science Letters, v. 111, no. 1, p. 1-10.

Idnurm, M. and B.R. Senior 1978. Palaeomagnetic ages of Late Cretaceous and Tertiary weathered profiles in the Eromanga Basin, Queensland. Palaeogeography, Palaeoclimatology, Palaeoecology, v. 24, no. 4, p. 263-277.

Irving, E. and L.G. Parry 1963. Magnetism of some Permian rocks from New South Wales. Geophysical Journal, v. 7, no. 4, p. 395-411.

Irving, E. 1977. Drift of the major continental blocks since the Devonian. Nature, v. 270, p. 304-309.

Jenny, J. and G. Stampfli 1978. Lithostratigraphie du Permien de l'Elbourz oriental en Iran. Eclogae geologicae Helveticae, v. 71, no. 3, p. 551-580.

Khramov, A.N. 1982. Paleomagnetic directions and pole positions: Data for the USSR. Soviet Geophysical Committee, World Data Center-B (Moscow), Issue 5, Catalogue.

King, R.F. and A.I. Rees 1966. Detrital magnetism in sediments: An examination of some theoretical models. Journal of Geophysical Research, v. 71, p. 561-571.

Kirschvink, J.L. 1980. The least-squares line and plane and the analysis of palaeomagnetic data. Geophysical Journal of the Royal Astronomical Society, v. 62, no. 3, p. 699-718.
Klootwijk, C.T. and D.K. Bingham 1980. The extent of Greater India, III. Palaeomagnetic data from the Tibetan sedimentary series, Thakkhola Region, Nepal Himalaya. Earth and Planetary Science Letters, v. 51, no. 2, p. 381-405.
Leven, E.J., M. Gaetani and S. Schroeder 2007. New findings of Permian fusulinids and corals from western Karakorum and E Hindu Kush (Pakistan). Rivista Italiana di Paleontologia e Stratigrafia, v. 113, no. 2, p. 151-165.
Lottes, A.L. and D.B. Rowley 1990. Reconstruction of the Laurasian and Gondwanan segments of Permian Pangaea. In W.S. McKerrow and C.R. Scotese (Eds.), Palaeozoic, Palaeogeography and Biogeography. Geological Society of London, Memoir, v. 12, p. 383-395.
Lowrie, W. 1990. Identification of ferromagnetic minerals in a rock by coercivity and unblocking temperature properties. Geophysical Research Letters, v. 17, p. 159-162.
Matte, P. 2001. The Varisican collage and orogeny (480–290 Ma) and the tectonic definition of the Armorica microplate: A review. Terra Nova, v. 13, p. 122-128.
McElhinny, M.W., C.M. Powell and S.A. Pisarevsky 2003. Paleozoic terranes of eastern Australia and the drift history of Gondwana. Tectonophysics, v. 362, no. 1, p. 41-65.
McKenzie, D.P. and W.J. Morgan 1969. Evolution of triple junctions. Nature, v. 224, p. 125-133.
Meert, J.G.L., R. Van der Voo, C.M. Powell, Z.-X. Li, M.W. McElhinny, Z. Chen and D.T.A. Symons 1993. A plate-tectonic speed limit? Nature, v. 363, p. 216-217.
Menning, M., A.S. Alekseev, B.I. Chuvashov, V.I. Davydov, F.-X. Devuyst, H.C. Forke, T.A. Grunt, L. Hance, P.H. Heckel, N.G. Izokh, Y.-G. Jin, P.J. Jones, G.V. Kotlyar, H.W. Kozur, T.I. Nemyrovska, J.W. Schneider, X.-D. Wang, K. Weddige, D. Weyer and D.M. Work 2006. Global time scale and regional stratigraphic reference scales of Central and West Europe, East Europe, Tethys, South China, and North America as used in the Devonian – Carboniferous – Permian Correlation Chart 2003 (DCP 2003). Palaeogeography, Palaeoclimatology, Palaeoecology, v. 240, no. 1-2, p. 318-372.
Metcalfe, I. 2002. Permian tectonic framework and palaeogeography of SE Asia. Journal of Asian Earth Sciences, v. 20, no. 6, p. 551-566.
Metcalfe, I. 2006. Palaeozoic and Mesozoic tectonic evolution and palaeogeography of East Asian crustal fragments: The Korean Peninsula in context. Gondwana Research, v. 9, p. 24-46.
Morel, P. and E. Irving 1981. Paleomagnetism and the evolution of Pangea. Journal of Geophysical Research, v. 86, no. B3, p. 1858-1987.
Muttoni, G., D.V. Kent and J.E.T. Channell 1996. Evolution of Pangea: Paleomagnetic constraints from the Southern Alps, Italy. Earth and Planetary Science Letters, v. 140, no. 1, p. 97-112.
Muttoni, G., D.V. Kent, E. Garzanti, P. Brack, N. Abrahamsen and M. Gaetani 2003. Early Permian Pangea 'B' to Late Permian Pangea 'A'. Earth and Planetary Science Letters, v. 215, no. 3, p. 379-394.
Muttoni, G., D.V. Kent, E. Garzanti, P. Brack, N. Abrahamsen and M. Gaetani 2004. Erratum to "Early Permian Pangea 'B' to Late Permian Pangea 'A'": [Earth and Planetary Science Letters, v. 215, no. 3, p. 379-394]. Earth and Planetary Science Letters, v. 218, no. 3, p. 539-540.
Muttoni, G., M. Mattei, M. Balini, A. Zanchi, M. Gaetani and F. Berra 2009. The drift history of Iran from the Ordovician to the Triassic. In M.-F. Brunet, M. Wilmsen and J.W. Granath (Eds.), South Caspian to Central Iran Basins. Geological Society of London Special Publication no. 312, in press.
Nawrocki, J. 1997. Permian to Early Triassic magnetostratigraphy from the Central European Basin in Poland: Implications on regional and worldwide correlations. Earth and Planetary Science Letters, v. 152, no. 1, p. 37-58.
Nawrocki, J., M. Kuleta and S. Zbroja 2003. Buntsandstein magnetostratigraphy from the northern part of the Holy Cross Mountains. Geological Quarterly, v. 47, no. 3, p. 253-260.
Rochette, P. and D. Vandamme 2001. Pangea B: An artifact of incorrect paleomagnetic assumptions? Annali di Geofisica, v. 44, no. 3, p. 649-658.
Ruban, D.A., M.I. Al-Husseini and Y. Iwasaki 2007. Review of Middle East Paleozoic plate tectonics. GeoArabia, v. 12, no. 3, p. 35-56.
Ruttner, A.W. 1993. Southern borderland of Triassic Laurasia in northeast Iran. Geologische Rundschau, v. 82, no. 1, p. 110-120.
Schaltegger, U. and P. Brack 2007. Crustal-scale magmatic systems during intra-continental strike-slip tectonics: U, Pb and Hf isotopic constraints from Permian magmatic rocks of the Southern Alps. International Journal of Earth Sciences, v. 96, no. 6, p. 1131-1151.
Schmidt, P.W. and B.J.J. Embleton 1976. Palaeomagnetic results from sediments of the Perth Basin, Western Australia, and their bearing on the timing of regional lateritisation. Palaeogeography, Palaeoclimatology, Palaeoecology, v. 19, no. 4, p. 257-273.

Schmidt, P.W., V. Prasad and P.K. Ramam 1983. Magnetic ages of some Indian laterites. Palaeogeography, Palaeoclimatology Palaeoecology, v. 44, no. 3-4, p. 185-202.

Schmidt, P.W. and C.D. Ollier 1988. Palaeomagnetic dating of Late Cretaceous to Early Tertiary Weathering in New England, N.S.W., Australia. Earth-Science Reviews, v. 25, no. 5-6, p. 363-371.

Scotese, C.R. 2001. Atlas of Earth History, Volume 1, Paleogeography, PALEOMAP Project, Arlington, Texas. v. 1, 52 p.

Sengör, A.M.C. 1979. Mid-Mesozoic closure of Permo-Triassic Tethys and its implications. Nature, v. 279, p. 590-593.

Seyed-Emami, K. 2003. Triassic in Iran. Facies, v. 48, no. 1, p. 91-106.

Shi, G.R., N.W. Archbold and L.-P. Zhan 1995. Distribution and characteristics of mid-Permian (Late Artinskian-Ufimian) mixed/transitional marine faunas in the Asian region and their palaeogeographical implications. Palaeogeography, Palaeoclimatology, Palaeoecology, v. 114, no. 2, p. 241-271.

Shi, G.R. and N.W. Archbold 1998. Permian marine biogeography of SE Asia. In R. Hall and J.D. Holloway (Eds.), Biogeography and Geological Evolution of SE Asia, p. 57–72. Backhuys Publishers, Leiden, The Netherlands.

Shi, G.R. 2006. Marine Permian of East and NE Asia: An overview of biostratigraphy, palaeobiogeography and implications for palaeogeography and plate tectonics. Journal of Asian Earth Sciences, v. 26, no. 3-4, p. 175-206.

Spring, L., F. Bussy, J.-C. Vannay, S. Huon and M.A. Cosca 1993. Early Permian granitic dykes of alkaline affinity in the Indian High Himalaya of Upper Lahul and SE Zanskar: Geochemical characterization and geotectonic implications. In P.J. Treloar and M.P. Searle (Eds.), Himalayan tectonics. Geological Society of London, Special Publications, v. 74, p. 251-264.

Stampfli, G. and G.D. Borel 2002. A plate tectonic model for the Paleozoic and Mesozoic constrained by dynamic plate boundaries and restored synthetic oceanic isochrons. Earth and Planetary Science Letters, v. 196, no. 1, p. 17-33.

Stöcklin, J. 1968. Structural history and tectonics of Iran: A review. American Association of Petroleum Geologists Bulletin, v. 52, no. 7, p. 1229-1258.

Stöcklin, J. 1974. Possible ancient continental margins in Iran. In C.A. Burk and C.L. Drake (Eds.), The Geology of Continental Margins, Springer-Verlag, p. 873-887.

Szurlies, M., G.H. Bachmann, M. Menning, N.R. Nowaczyk and K.-C. Käding 2003. Magnetostratigraphy and high-resolution lithostratigraphy of the Permian – Triassic boundary interval in Central Germany. Earth and Planetary Science Letters, v. 212, no. 3, p. 263-278.

Tauxe, L. and D.V. Kent 1984. Properties of a detrital remanence carried by haematite from study of modern river deposits and laboratory redeposition experiments. Geophysical Journal of the Royal Astronomical Society, v. 76, no. 3, p. 543-561.

Théveniaut, H. and P. Freyssinet 1999. Paleomagnetism applied to lateritic profiles to assess saprolite and duricrust formation processes: The example of Mont Baduel profile (French Guiana). Palaeogeography, Palaeoclimatology, Palaeoecology, v. 148, no. 4, p. 209-231.

Théveniaut, H. and P. Freyssinet 2002. Timing of lateritization on the Guiana Shield: Synthesis of paleomagnetic results from French Guiana and Suriname. Palaeogeography, Palaeoclimatology, Palaeoecology, v. 178, no. 1, p. 91-117.

Torq, F., J. Besse, D. Vaslet, J. Marcoux, L.E. Ricou, M. Halawani and M. Basahel 1997. Paleomagnetic results from Soudi Arabia and the Permo-Triassic Pangea configuration. Earth and Planetary Science Letters, v. 148, no. 3-4, p. 553-567.

Torsvik, T.H. and R. Van der Voo 2002. Refining Gondwana and Pangea palaeogeography: Estimates of Phanerozoic non-dipole (octupole) fields. Geophysical Journal International, v. 151, no. 3, p. 771-794.

Torsvik, T.H. and L.R.M. Cocks 2004. Earth geography from 400 to 250 Ma: A palaeomagnetic, faunal and facies review. Journal of the Geological Society of London, v. 161, no. 4, p. 555-572.

Van der Voo, R. 1993. Paleomagnetism of the Atlantic, Tethys and Iapetus Oceans. Cambridge University Press, Cambridge, 411 p.

Van der Voo, R. and T.H. Torsvik 2001. Evidence for late Paleozoic and Mesozoic non-dipole fields provides an explanation for the Pangea reconstruction problems. Earth and Planetary Science Letters, v. 187, no. 1, p. 71-81.

Van Houten, F.B. 1982. Ancient soils and ancient climates, climate in Earth history: Studies in geophysics. Geophysics Study Committee, Geophysics Research Board, Commission on Physical Sciences, Mathematics, and Applications, National Research Council, 212 p.

Wellman, H.W. 1965. Active wrench faults of Iran, Afghanistan and Pakistan. Geologische Rundschau, v. 53, no. 3, p. 716-735.
Wendt, J., B. Kaufmann, Z. Belka, N. Farsan and A.K. Bavandpur 2005. Devonian/Lower Carboniferous stratigraphy, facies patterns and palaeogeography of Iran Part II. Northern and central Iran. Acta Geologica Polonica, v. 55, no. 1, p. 31-97.
Wensink, H. 1979. The implications of some palaeomagnetic data from Iran for its structural history. Geologie en Mijnbouw, v. 58, 175 p.
Zanchi, A., M. Gaetani and S. Sironi 2007, The new geological map of Central-Western Karakoram. Rendiconti della Società Geologica Italiana, v. 4, p. 315-318.
Zanchi, A., S. Zanchetta, E. Garzanti, M. Balini, F. Berra, M. Mattei and G. Muttoni 2009a. The Cimmerian evolution of the Nakhlak–Anarak area, central Iran, and its bearing for the reconstruction of the history of the Eurasian margin. In M.-F. Brunet, M. Wilmsen and J.W. Granath (Eds.), South Caspian to Central Iran Basins. Geological Society of London Special Publication no. 312, in press.
Zanchi, A., S. Zanchetta, F. Berra, M. Mattei, E. Garzanti, S. Molyneux, A. Nawab and J. Sabouri 2009b. The Eo-Cimmerian (Late? Triassic) orogeny in north Iran. In M.-F. Brunet, M. Wilmsen and J.W. Granath (Eds.), South Caspian to Central Iran Basins. Geological Society of London Special Publication no. 312, in press.
Zaninetti, L., P. Brönnimann, F. Bozorgnia and H. Huber 1972. Etude lithologique et micropaléontologique de la formation d'Elikah dans la coupe d'Aruh, Alborz Central, Iran septentrional. Archives des Sciences de Genève, v. 25, no. 2, p. 215-249.
Ziegler, A.M., G. Eshel, P. McAllister Rees, T.A. Rothfus, D.B. Rowley and D. Sunderlin 2003. Tracing the tropics across land and sea: Permian to present. Lethaia, v. 36, no. 3, p. 227-254.
Zijderveld, J.D.A. 1967. A.C. demagnetization of rocks - analysis of results. In D.W. Collinson, K.M. Creer and S.K. Runcorn (Eds.), Methods in Paleomagnetism, Elsevier, New York, p. 254-286.

ABOUT THE AUTHORS

Giovanni Muttoni *is an Associate Professor of Stratigraphy at the Department of Earth Sciences, University of Milan, Italy. He received a PhD in Magnetostratigraphy from the University of Milan in 1994; he was Post-doctoral Fellow at Lamont-Doherty Earth Observatory of Columbia University, USA, in 1994-1995, Post-doctoral Fellow at the Institute of Marine Geology, C.N.R. Bologna, Italy, in 1995-1997, and Wissenschaft Assistant at the Institute of Geophysics, ETH Zurich, Switzerland, in 1997-2000. Since 2000, he is at the University of Milan. His present research interests are Permian-Triassic paleogeography and time scales, and Eocene and Pleistocene stratigraphy and climate change.*

giovanni.muttoni1@unimi.it

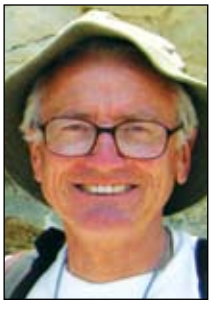

Maurizio Gaetani *is Professor of Geology at the University of Milano. He has 40 years of field activity in the Alps, eastern Mediterranean (Albania, Greece - Chios, Hydra), around the Caspian (northwest Caucasus, Mangyshlak, Turkmenistan, northern Iran) and in the Karakorum-Western Himalaya (Pakistan, India). Maurizio is co-leader of the research programs: Peri-Tethys and Middle East Basin Evolution, and is former Chairman of the IUGS Subcommission on Triassic Stratigraphy. He is also Editor of the Rivista Italiana di Paleontologia e Stratigrafia. Maurizio's main research interests include the stratigraphy of Permian and Triassic, and paleogeographic reconstructions for the same interval.*

maurizio.gaetani@unimi.it

Dennis V. Kent *is Board of Governor's Professor of Geological Sciences at Rutgers University in Piscataway, New Jersey, and Adjunct Senior Research Scientist at Lamont-Doherty Earth Observatory in Palisades, New York. He has published widely on the tempo of geomagnetic polarity reversals, paleogeographic reconstructions, and other topics related to Earth magnetism. His current research interests include Triassic and Jurassic magnetostratigraphy and astronomical polarity time scales; the relationship of tectonics, paleoclimates and the carbon cycle; and the magnetic recording properties of sediments and oceanic basalts. Kent is a fellow of the AGU, GSA, and AAAS and a member of the U.S. National Academy of Sciences.*

dvk@rutgers.edu

Dario Sciunnach *obtained his PhD on Himalayan stratigraphy from the University of Milan, Italy. He has worked for ten years at Regione Lombardia on the Italian program of Geological CARtography at the 1:50,000 scale (CARG). His disciplinary interests include geological mapping, physical stratigraphy, sandstone petrography, heavy-mineral geochemistry and basin analysis. He has cooperated with the Milan universities, the Italian Stratigraphic Commission, the National Research Council and ENI, on projects in sedimentary geology (Alpine-Himalayan orogen, Po Plain subsurface); stratigraphic nomenclature; and geotourism, both in Lombardy and in the Cape Verde Islands.*

dario_sciunnach@regione.lombardia.it

Lucia Angiolini *is a Professor of Palaeontology at the Department of Earth Sciences, University of Milano, Italy. She received a PhD in Earth Sciences from University of Milan in 1994, where she is now Associate Professor of Palaeontology. Lucia has 15 years experience in Permian brachiopods from the Peri-Gondwana region and the Cimmerian blocks from Turkey to the Himalayas through Oman, Iran and Karakorum. Her research interests include, besides pure taxonomy, quantitative biostratigraphy, palaeobiogeography based on multivariate analyses, and Permian correlation between Gondwanan and Tethyan realms.*

lucia.angiolini@unimi.it

Fabrizio Berra *is Researcher at the Department of Earth Sciences at the University of Milan, Italy. He started his career working on the stratigraphy and paleogeography of the Late Triassic successions of the Alps since his PhD (1994). He worked on the new Geological Map of Italy before joining the University (2002), both on field survey and GIS database. His research is mainly focused on the stratigraphy of the Southern Alps, Sardinia, Iran and the Himalayas, as well as on the basin analyses. In particular, his research mainly deals with Mesozoic carbonate systems and on the controls exerted by climate, eustatic and tectonics on their evolution.*

fabrizio.berra@unimi.it

Eduardo Garzanti *is a full Professor of Stratigraphy at the University of Milan-Bicocca, Italy. He has a long experience in the geology of the Himalayas (India/Asia collision, Indian foreland basin, Transhimalaya forearc basin, Tethys Himalayan passive margin, Opening of Neo-Tethys, Paleozoic orogeny). His work is mainly focused on provenance models inferred from analysis of both detrital modes and dense mineral suites of Tertiary to modern sediments issued from the Alpine-Himalayan Orogen; most recent work includes the petrographic and mineralogical study of modern sands in the Indus and Ganga-Brahmaputra river systems, and of Tertiary terrigenous successions in the Himalayan foreland basin from Pakistan to India, Nepal, Bangladesh, Myanmar, and the Andaman Islands. He has also active research projects in Northern Africa (petrographic, mineralogical, geochemical, and isotopical signatures of the Main Nile, Blue Nile and White Nile) and Central Africa (chemical weathering of detritus in tropical climates), and on modern sand seas (Nafud, Dahna, Jafurah and Rub Al Khali in Arabia and Namib in Southerrn Africa). His most recent attention is on mineralogical and chemical variability of modern sediments in big fluvio-deltaic systems worldwide.*

eduardo.garzanti@unimib.it

Massimo Mattei *is Associate Professor of Structural Geology at the Department of Geological Sciences, University of Roma TRE, Italy. He received a PhD in Structural Geology from Roma "La Sapienza" University in 1992. Massimo has 15 years experience in paleomagnetism and tectonics in the Mediterranean region, Ande, and Iran. His research interest include the origin and tectonic evolution of curved orogens, structural evolution of back-arc basins, emplacement mechanism of pyroclastic flows, magnetic fabric of weakly deformed sediments.*

mattei@uniroma3.it

Andrea Zanchi *received his PhD in 1989 from the University of Milan, Italy, on fault analysis and paleostress reconstruction, working on the opening of the Gulf of California. His research interests mainly concern the structural analysis and mapping of poorly-known Asian Meso-Cenozoic orogenic belts, (Karakoram, Pakistan; Alborz, Iran). He had also worked on the Chios Palaeozoic accretionary complex and on the recent evolution of Syria. He participated to several International projects (Ev-K2, GETS, ALARM, Peri-Tethys, and MEBE). He is a Professor in structural geology at the University of Milano-Bicocca in the Department of Geological Sciences and Geotechnologies.*

andrea.zanchi@unimib.it

Manuscript received November 18, 2008

Revised February 19, 2009

Accepted February 22, 2009

Press version proofread by authors July 6, 2009